FINAL

**WORKPLAN:
HYDROLOGIC MODEL OF THE
UPPER WATERSHED OF
THE EAST FORK OF THE
SOUTH FORK OF THE SALMON RIVER,
STIBNITE, IDAHO**

prepared by

Erwin A. Melis, PhD, PG

(CA No. 8870; ID PGL-1582)

Michael A. Jones

Jacob Baggerman

JOHN SHOMAKER & ASSOCIATES, INC.
Water-Resource and Environmental Consultants
2611 Broadbent Parkway NE
Albuquerque, New Mexico, 87107 USA
505-345-3407
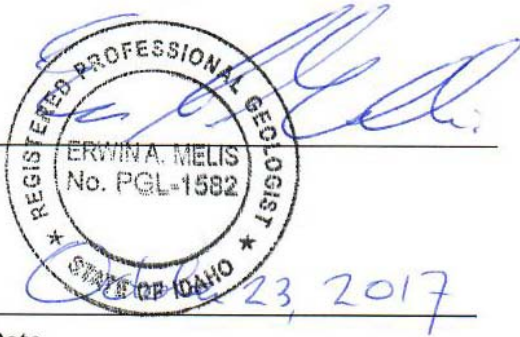www.shomaker.com

for

Midas Gold Idaho, Inc.
Boise, Idaho

October 23, 2017
⍰⍰

Professional Geologist Seal

This report documents work conducted by, or overseen, reviewed and approved by, the following Idaho Professional Geologist:

Erwin A. Melis, PhD, PGL-1582

Date

WORKPLAN: HYDROLOGIC MODEL OF THE UPPER WATERSHED OF THE EAST FORK OF THE SOUTH FORK OF THE SALMON RIVER, STIBNITE, IDAHO

EXECUTIVE SUMMARY

This report presents the workplan directing the mathematical model of the hydrologic system of the upper watershed of the East Fork of the South Fork of the Salmon River in north-central Idaho, where Midas Gold Idaho, Inc. proposes the Stibnite Gold Project (Project).

The Project involves development of open pits, development rock storage facilities, processing plant, and tailings storage facility. These necessitate diversion of groundwater and surface water and consumption and discharge of water, potentially resulting in effects on downstream flow and water quality, and local effects on groundwater levels, stream flows, and water quality in the watershed.

Precipitation on the forested, high-altitude watershed occurs mostly as winter snow which melts in spring and early summer, and averages about 30 inches per year. The melt is partly consumed by vegetation in the watershed, while the rest becomes flow in the river. Local groundwater bodies store melt water and gradually transmit it to the river, providing year-round baseflow.

The model combines a long-term meteoric water balance tracking precipitation, snow accumulation and melt, with a numerical model of groundwater and surface water flow. The result is a model of groundwater and surface water flows reflecting a range of wet and dry climatic conditions with the associated frequencies of occurrence.

The model will be used to:

- Estimate dewatering rates required to develop the open pit mines.

- Estimate ranges of surface and groundwater flows at different locations, under different conditions and at different phases of mining and post-closure, to support site-wide water-balance and water-quality modeling.

- Estimate the local effects of dewatering and water management strategies on groundwater levels and stream flows.

- Project post-mining open pit filling and pit water balances.

- Provide water balance inputs to the evaluation of the downstream effects of the Project (potential changes in EFSFSR flow and water quality).

This work plan presents the site hydrology and hydrogeology and a conceptual model of the overall hydrologic system. The model structure and inputs are then presented along with model development and calibration. Projection of the hydrologic effects of the Project, will be developed in cooperation with agencies and stakeholders and will be reported separately.

TABLE OF CONTENTS

LIST OF FIGURES

LIST OF TABLES

LIST OF ABBREVIATIONS

DEM   digital elevation model

DRSF   development rock storage facility

EFSFSR   East Fork of the South Fork of the Salmon River

ft amsl   feet above mean sea level

JSAI   John Shomaker & Associates, Inc.

PRO   Plan of Restoration and Operations

RMSE   root-mean squared error

TSF   tailings storage facility

WRSR   Water Resources Summary Report

WORKPLAN: HYDROLOGIC MODEL OF THE UPPER WATERSHED OF THE EAST FORK OF THE SOUTH FORK OF THE SALMON RIVER, STIBNITE, IDAHO

1.0 INTRODUCTION

John Shomaker & Associates, Inc. (JSAI) was contracted by Midas Gold Idaho, Inc. (Midas Gold) to prepare a hydrologic model for the Stibnite Gold Project (Project) study area. The study area, shown on Figure 1.1, is the upper watershed of the East Fork of the South Fork of the Salmon River (EFSFSR) in Valley County, Idaho, in the Stibnite mining district.
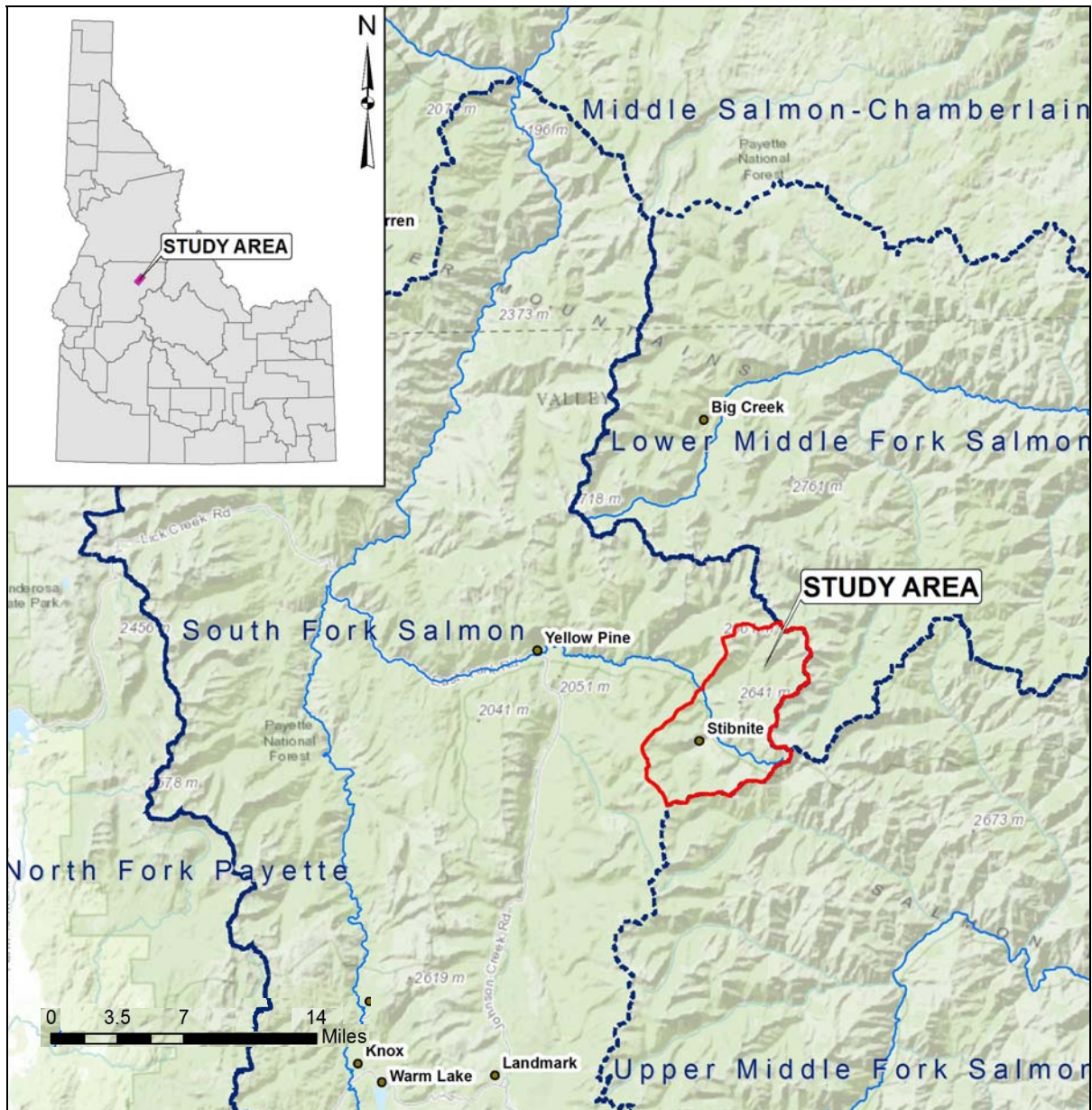
Figure 1.1. Location map of the Stibnite Project, Valley County, Idaho.

The hydrologic/hydrogeologic model will provide flow inputs to a related site-wide water management model that will be used to evaluate the complex interaction of fresh water, process water, tailings water and contact water entering and exiting the different mine facilities. Water management activities considered in the site-wide water management model include groundwater withdrawals, surface water collection and conveyance, water storage, enhanced evaporation, water treatment and excess water release to the stream system.

The model will also provide input to a related set of water-quality models that evaluate the water chemistry of the open pits, the groundwater and surface water quality down-gradient of other Project facilities, and the water quality in the EFSFSR downstream of the Project.

A final model of the hydrologic system will be prepared by JSAI in cooperation with agencies and stakeholders to evaluate potential hydrologic effects of the Project. This work plan incorporates information related to the understanding of the system accumulated and developed by Midas Gold and outlines the conceptual model and computational framework guiding JSAI model development.

1.1 Site Background and Project Plan

The study area is a mountain watershed dominated by winter snow accumulation and spring/summer melt. A network of stream channels drains snowmelt and rainfall from the mountain block, where locally groundwater is stored and provides year-round base flow to streams.

The area has been a mining district since the late 19th century. Mining occurred intermittently from the 1890s through the 1990s, with major operations in the 1920s through early 1950s and from the late 1970s through the 1990s.

Existing legacy mining facilities include a tailings impoundment and a spent-ore disposal area along Meadow Creek, the Yellow Pine open pit along the EFSFSR, and various adits, tunnels and other underground workings, heap leach pads, rock dumps, and smaller pits throughout the study area. Midas Gold began exploration activities in the area in 2009.

The anticipated life of the Project is approximately 20 years, including approximately 3 years for site cleanup, infrastructure construction, and early restoration activities; 12 to 15 years for operations; and 2 to 3 years for final closure and reclamation work. Details of the proposed plan are provided in the Project Plan of Restoration and Operations (PRO; Midas Gold, 2016).

The PRO consists of two primary components: (1) restoration of major legacy impacts from historical mining activities, and (2) redevelopment of open-pit mining and reclamation of the three primary ore deposit areas: Yellow Pine pit in the north area, West End pit in the northeast area, and Hangar Flats pit in the southern area.

The site, with proposed new facilities, is shown on Figure 1.2. The EFSFSR and tributaries include Meadow Creek, site of an historical tailings storage facility (TSF) and a spent-ore deposit area, and the location of the proposed Hangar Flats pit, Hangar Flats development rock storage facility (DRSF), and proposed TSF.

The proposed Yellow Pine pit is an expansion of the historical Yellow Pine pit, located in the main reach of the EFSFSR. The Fiddle DRSF is located in the Fiddle Creek valley. The proposed West End pits and the proposed West End DRSF are located in the West End Creek valley (Fig. 1.2).

Hangar Flats pit is planned to be excavated to a depth of approximately 610 feet below the elevation of Meadow Creek. The pit will be partly excavated in saturated alluvium along Meadow Creek. Dewatering of the alluvium will be required during mining to provide for dry mining conditions and to provide water supply for mining and ore processing activities. A proposed lined diversion channel is planned to route Meadow Creek around the TSF, the DRSF and the Hangar Flats pit. Post closure, the open pit would fill and the diversion channel is planned to be re-configured to route Meadow Creek through the pit lake.

The Yellow Pine pit would be an expansion of the existing open pit through which the EFSFSR flows and is also planned to be excavated to a depth of approximately 610 feet below the elevation of the EFSFSR at the rim of the existing pit. A tunnel is proposed to route the EFSFSR around the expanded pit during mining operations. Post closure, the Yellow Pine pit would be backfilled and the EFSFSR restored over the surface of the fill.

The West End pit would reach approximately 400 feet depth below West End Creek and would require diverting West End Creek and would. Post closure, the open pit would fill and West End Creek would flow through the pit lake.
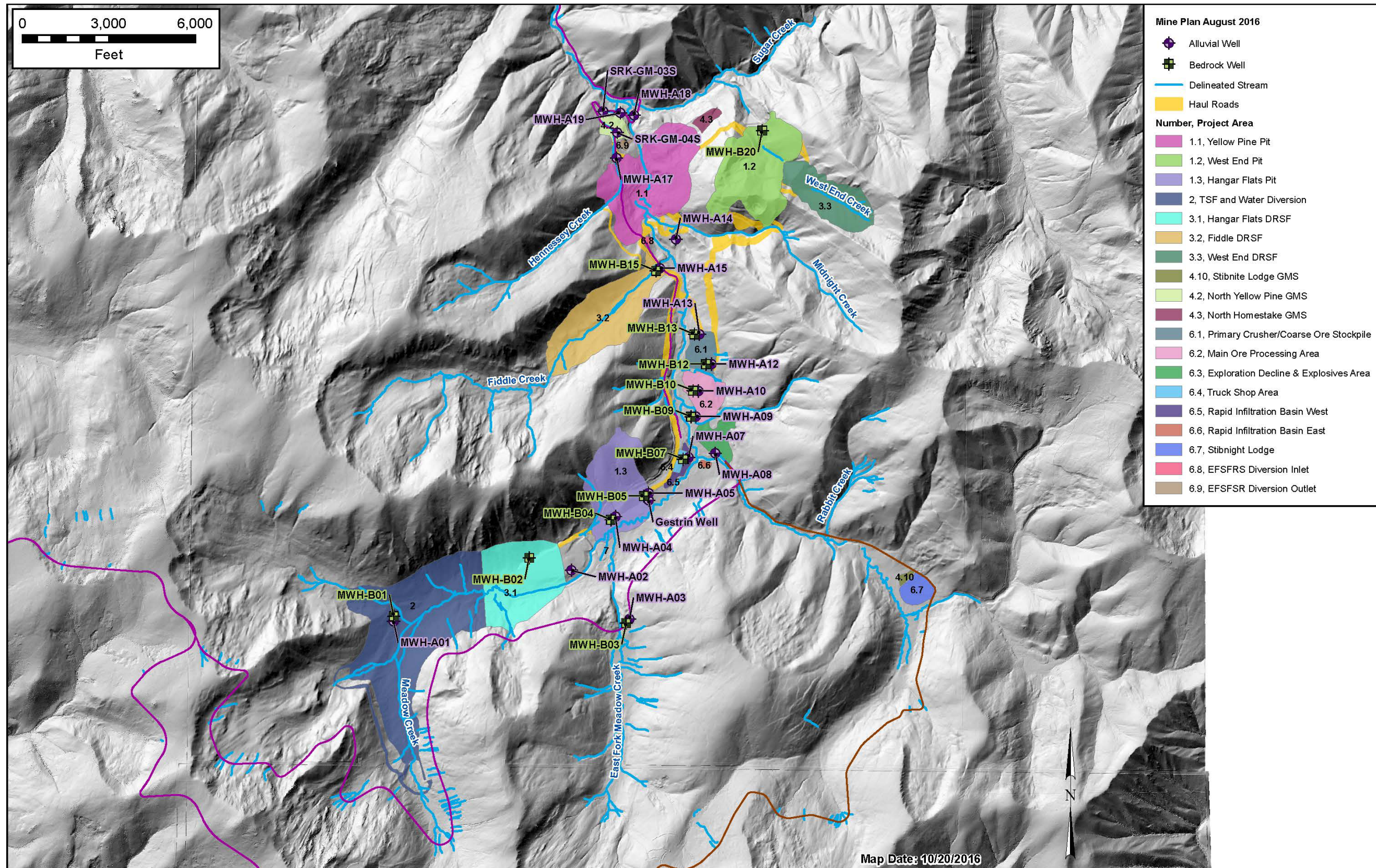
Figure 1.2. Project features.

1.2 Statement of Need

The Project will involve dewatering of open pits, diversion of surface flows, use of water for ore processing and milling, and discharge of treated excess water to the groundwater and/or stream system. A quantitative understanding of the hydrologic/hydrogeologic system is needed for the following purposes:

- Estimate dewatering requirements,

- Design water-conveyance infrastructure capacity,

- Evaluate availability of water supply

- Size water storage and treatment infrastructure

- Evaluate the effects of mine-related activities on water levels and stream flows

- Provide input to water-quality modeling, water management evaluation and other assessments as necessary

Because annual precipitation in the study area is highly variable, the hydrologic model will quantify the range of flows that may occur under a range of expected climatic conditions, and their frequency of occurrence.

1.3 Modeling Objectives

The model considers the elements of the hydrologic conceptual site model and available information as detailed in the Water Resources Summary Report (WRSR, Brown and Caldwell [BC], 2017) and includes the following steps:

- Develop a meteoric water balance tracking monthly precipitation, snow accumulation, sublimation/evaporation, and melt, to estimate runoff and recharge inputs to the surface water and groundwater flow model.

- Develop a numerical model of surface water and groundwater flow in the study area.

- Calibrate the combined water balance and numerical model to closely resemble measured surface water flow rates, groundwater levels, and aquifer test results.

The calibrated hydrologic model will be used to:

- Estimate dewatering rates required to develop the open pit mines.

- Estimate the local effects of dewatering and water management strategies on groundwater levels and stream flows.

- Estimate water balances, and ranges of surface water and groundwater flows at different locations and for different mine facility footprints, including:

    - Open-pit post-mining filling rates and water balances

- Water balances for Development Rock Storage Facility footprints
- Water balance for Tailings Storage Facility footprint
- Flow and water balances for stream flow monitoring points

The water balances computed using the hydrologic model in turn provide flow inputs to (a) the Site-Wide Water Balance model for Project facilities and flows of freshwater, process water, tailings water and other contact water illustrated on Figure 1.3 (from Midas Gold, 2016, figure 8-7) and (b) water-quality assessments for Project facilities and monitoring points.

Evaluation of potential Project effects on downstream flow and water quality in the EFSFSR will be based on combined results of the hydrologic model, the site-wide water management model, and the water-quality models. The flow of information from the different models used to evaluate the effects of the Project is illustrated on Figure 1.4.
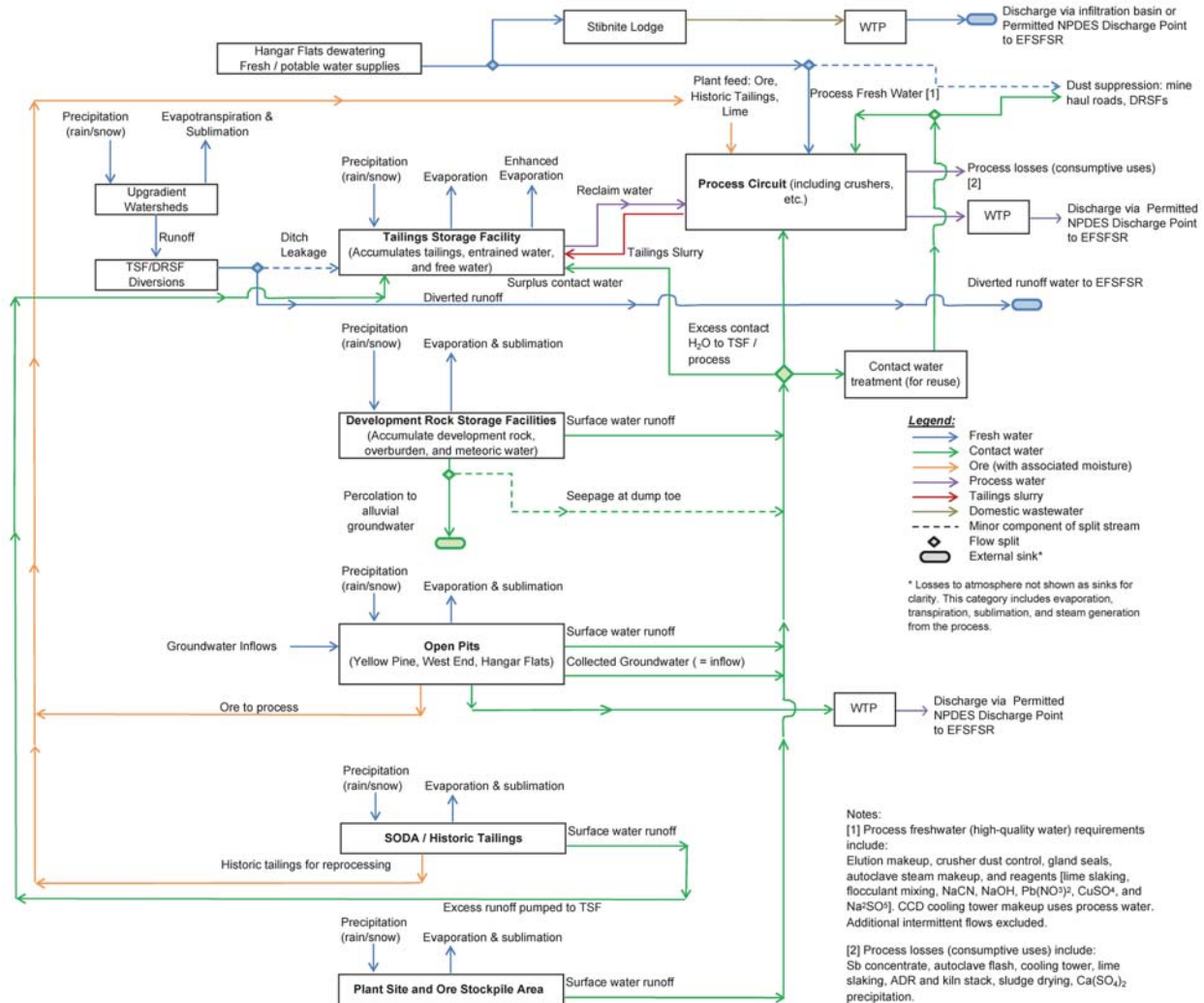
Figure 1.3. Water balance flow diagram (Midas Gold, 2016; figure 8-7).
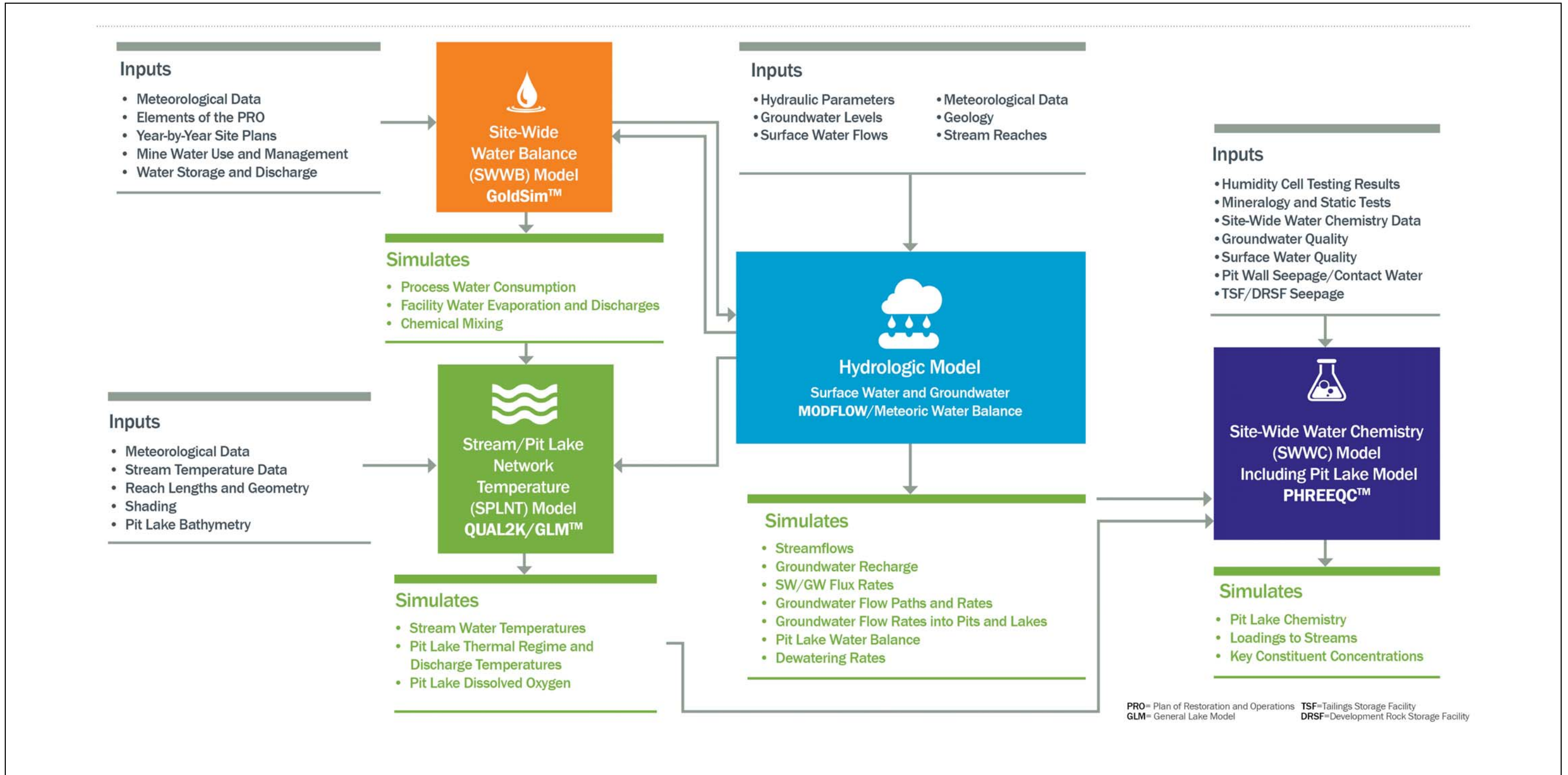
Figure 1.4. Project modeling process diagram.

2.0 HYDROLOGIC CONCEPTUAL SITE MODEL

The study area is a mountain watershed, with hydrologic conditions dominated by the seasonal patterns of snow accumulation and melt. Snow accumulates throughout the winter and melts in spring and early summer. A part of the melt water is consumed by vegetation in the watershed, while the larger part becomes flow in the EFSFSR.

The spring melt slowly drains to the EFSFSR, attenuated by surface topography and by the permeable layer of soil, colluvium, and alluvium that covers the crystalline bedrock over most of the area, and by evapotranspiration from the heavily vegetated watershed.

Part of the melt water circulates through local groundwater systems in alluvium and rock fractures that lie along the EFSFSR and its tributaries. The local groundwater systems store spring snow melt and discharge it to the stream system over the full year. Groundwater flows along and toward the surface channels, eventually entering the stream system.

The local groundwater systems generally function as extensions of the surface water system; they do not extend to great depth and are laterally restricted to the valley bottoms. The valley bottom groundwater flow systems are disconnected from each other by the mountains between them, and compartmentalized along the valley bottoms by bedrock constrictions.

The rock of the mountain-block study area consists of igneous and metamorphic crystalline rock units. There are no extensive geologic formations found that would normally form aquifers, such as sedimentary, carbonate or volcanic rock units. Groundwater flows in individual rock fracture networks, but there is no regional groundwater flow system connecting the local groundwater systems.

Elements of the study area hydrologic and hydrogeologic systems and the information available about them are presented in detail in the WRSR and summarized in the following sections discussing the local climate, surface water hydrology, and geology and groundwater hydrogeology of the study area. The final section summarizes the study area water balance.

2.1 Climate

The study area latitude is about 44.9 degrees north, with elevation ranging from about 5,900 feet above mean sea level (ft amsl) to about 8,400 ft amsl. The climate is characterized by cool summers and cold winters. Precipitation occurs mostly as winter snowfall, with the main input of water to the surface water and groundwater systems occurring during the spring melt.

Midas Gold has collected meteorological data in the study area since August 2011, including air temperature, barometric pressure, wind speed, and precipitation. Site data collection is ongoing and will continue through mine operations and post-closure.

Climate data for the region surrounding the study area were most recently reviewed by Tierra Group International, Ltd. (2013), utilizing regional National Weather Service Cooperative (COOP) meteorological stations, snowpack telemetry (SNOTEL) stations and pan evaporation stations.

The sections below summarize information and discuss (1) temperature and potential evaporation and (2) precipitation.

2.1.1 Temperature and Potential Evapotranspiration

Monthly average potential evapotranspiration has been estimated (Tierra Group International, Ltd, 2013) based on monthly average temperatures measured at site using the modified Blaney-Criddle method (Zhan and Shelp, 2009), then refined based on regional climate data. The estimates of monthly average temperature and potential evapotranspiration are presented in Table 2.1. Total annual potential evaporation is about 21 in./yr.

Table 2.1. Recorded site temperature and estimated potential evapotranspiration

month	average temperature, °F	modified Blaney-Criddle potential evapotranspiration, in.
Jan	20.1	0.7
Feb	21.8	0.8
Mar	27.7	1.3
Apr	32.9	1.6
May	40.7	2.3
June	48.7	2.7
July	58.1	3.3
Aug	56.5	3.0
Sept	48.7	2.2
Oct	39.2	1.5
Nov	26.3	0.9
Dec	18.8	0.7
annual		21.0

2.1.2 Precipitation

Precipitation is difficult to measure in the study area because (1) precipitation increases with elevation and (2) the spatial distribution of snow is highly uneven. In addition, snow gaging stations are technically difficult to maintain. Long-term records of precipitation are therefore sparse.

An analysis of long-term regional climate parameters, including precipitation, is provided by a "Parameter-elevation Regressions on Independent Slopes Model" (PRISM; *www.prism.oregonstate.edu*). The PRISM method interpolates a database of climate records onto a spatial grid covering the United States (Daly et al., 2008).

PRISM calculates a climate-elevation regression for each grid location based on data from nearby climate stations where long-term records are available, and on a digital elevation model (DEM). Factors considered in the regression used for interpolation of climate parameters include location, elevation, coastal proximity, topographic facet orientation, vertical atmospheric layer, topographic position, and orographic effectiveness of the terrain.

PRISM results include an estimate of monthly precipitation from 1895 through 2016 for grid cells in the study area. The 122-year series represents the best available estimate of long-term precipitation patterns and includes a range of wet, average, and dry conditions.

The statistical distribution of annual precipitation for the 122-year period is presented on Figure 2.1 for two grid cells in the Meadow Creek drainage basin (results for other nearby grid cells are similar). Annual precipitation ranges from about 20 to about 50 in., with a median of about 30 in./yr.
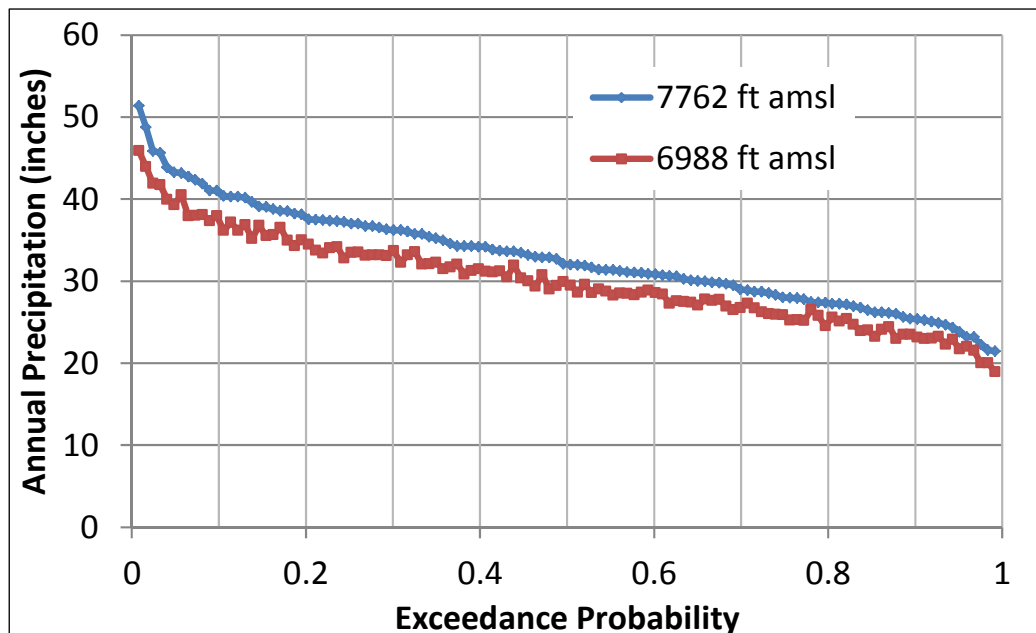
Figure 2.1. Distribution of annual precipitation.

While the long-term series shown on Figure 2.1 represent the time-variability and statistical distribution of precipitation, the regional-scale PRISM results do not consider stream flow gaging data available for the local study area. The monthly PRISM series is therefore modified in Section 2.5 below based on measured discharge rates, resulting in an elevation-weighted, basin average precipitation and in an estimate of the study area water balance.

2.2 Surface Water Hydrology

The sections below present (1) the stream network and surface drainage patterns and (2) surface flow monitoring points and flow measurements.

2.2.1 Stream Network

The EFSFSR stream network is shown on Figure 2.2, including the main EFSFSR channel and tributary streams including, among others, Meadow Creek, Fiddle Creek, and West End Creek. The area and elevation range of each sub-basin of the study area are listed on Table 2.2. The total drainage area is about 43 square miles (mi^2).

The full EFSFSR watershed area is about 422 mi^2 at the confluence with the South Fork Salmon River, with an estimated average annual discharge of about 435,000 acre-feet (HydroGeo, Inc., 2012), equivalent to a basin-average water yield of 19.3 in./yr.

Table 2.2. Watershed characteristics

ID	watershed name	area (mi^2)	minimum elevation	maximum elevation
1	Meadow Creek tributary	1.82	6,766	7,791
2	Blowout Creek	2.45	6,598	8,034
3	Meadow Creek	5.77	6,530	8,085
4	Upper EFSFSR	9.16	6,545	8,340
5	Middle EFSFSR/Garnet Creek	1.65	6,287	7,926
6	Middle EFSFSR/Fiddle Creek	2.04	6,279	7,755
7	Hennessy Creek	0.73	6,137	7,591
8	Midnight Creek	1.43	6,198	8,383
	Total EFSFSR above Sugar Creek	**25.05**	**5,929**	**8,383**
9	Sugar Creek	17.94	5,929	8,295
	Total	**43.0**	**5,929**	**8,383**

EFSFSR - East Fork of the South Fork of the Salmon River
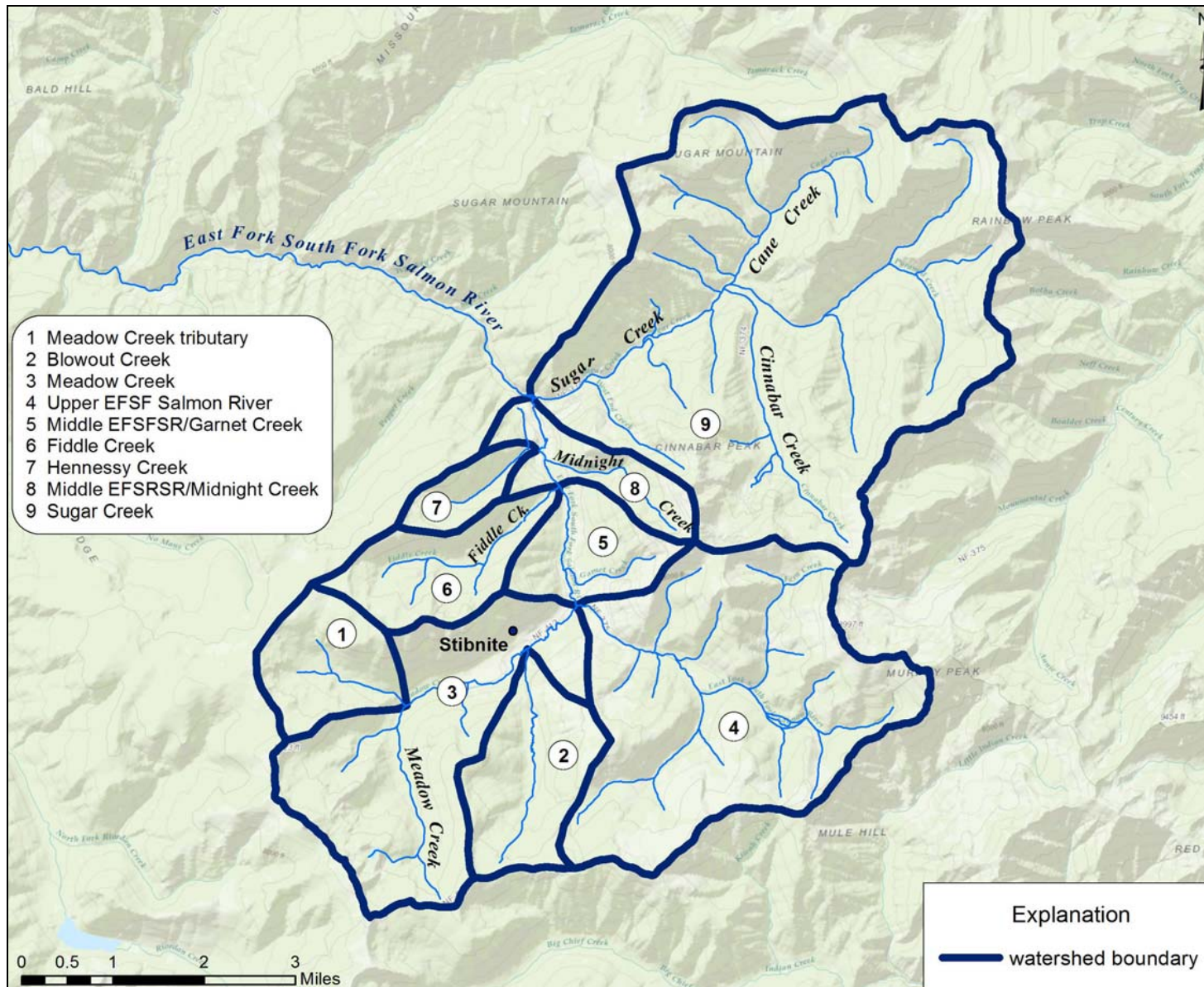
Figure 2.2. EFSFSR streams and sub-basins.

2.2.2 Surface Water Flow Rates

Locations of U.S. Geological Survey (USGS) streamflow gages within the study area are shown on Figure 2.3 along with mapped seeps and adit discharges monitored by Midas Gold since April 2012. USGS gages are summarized on Table 2.3. Flow at USGS gages is recorded continuously. Flow at the other sites is measured periodically, when water-quality samples are gathered.

Table 2.4 summarizes discharge rates measured at Midas Gold surface water quality monitoring points. Flows measured in the EFSFSR and the main tributaries are in line with flows measured at the USGS gages, presented below. Flows measured in the adits and seeps off the main channels are smaller, in rough proportion to the surface and underground drainage area flowing to each monitoring point.

Table 2.3. USGS surface flow gages

station	ID	elevation, ft amsl	upstream catchment area, mi^2
EFSFSR above Meadow Creek near Stibnite	13310800	6,546	9.2
Meadow Creek near Stibnite	13310850	6,639	5.5
EFSFSR at Stibnite	13311000	6,460	19.3
EFSFSR above Sugar Creek near Stibnite	13311250	5,944	25.1
Sugar Creek near Stibnite	13311450	5,950	17.9

ft amsl - feet above mean sea level

Historical streamflow data from 2011 through 2016 are shown for each USGS gage on Figures 2.4 through 2.13. Flows are generally characterized by peaks in May and June that are about an order of magnitude higher than base flow in August through February. Therefore, flows are shown on a linear scale (to better see the high flows) in the even-numbered figures and a logarithmic scale (to better see the low flows) in the odd-numbered figures.

The magnitude of peak flow is variable, depending on annual snowfall, but the timing of the annual peak (May) is generally consistent from year to year. The magnitude of base flow is more consistent from year to year than peak flows, indicating consistent groundwater recharge in both wet years and dry years.

The steadiness of measured base flows is consistent with the relatively high minimum dry year precipitation of about 20 in. (Fig. 2.1) providing normal groundwater recharge, but low surface runoff, in dry years.
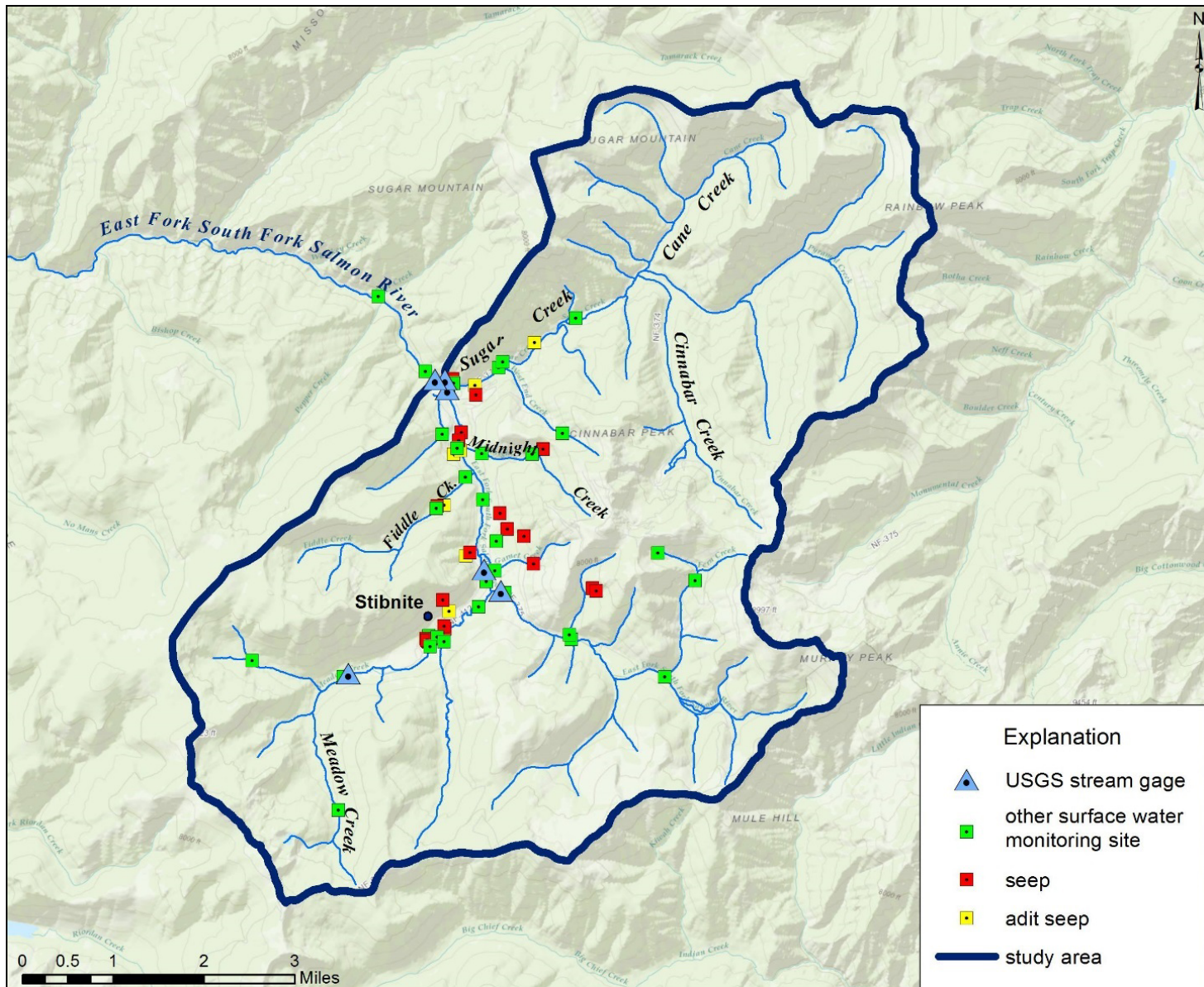
Figure 2.3. East Fork of the South Fork Salmon River watersheds and tributaries.

Table 2.4. Flow rates measured at Midas Gold surface water monitoring points

station	ID	measured discharge rate (cubic feet per second)
Monday Tunnel adit seep	YP-AS-3	4.5E-04 - 3.6E-02
Cinnabar Tunnel adit seep	YP-AS-4	4.0E-02 - 3.7E-01
North Tunnel adit seep	YP-AS-5	0.0E+00 - 6.2E-02
DMEA adit seep	YP-AS-6	1.8E-03 - 2.0E-02
Garnet Pit seep	YP-S-3	4.5E-03 - 1.7E-01
Old Haul Road seep	YP-S-9	1.6E-03 - 6.7E-03
North Bradley waste rock seep	YP-SEBS-1	1.1E-02 - 8.5E-02
South Bradley waste rock seep	YP-SEBS-2	1.8E-01 - 4.7E-01
EFSFSR below Meadow Creek	YP-SR-10	7.0E+00 - 1.7E+02
EFSFSR above Meadow Creek	YP-SR-11	4.0E+00 - 6.2E+01
EFSFSR uppermost site	YP-SR-13	3.0E+00 - 5.2E+01
EFSFSR above Fern Creek	YP-SR-14	8.0E-01
EFSFSR below Sugar Creek	YP-SR-2	9.0E+00 - 4.0E+02
EFSFSR below Yellow Pine Pit	YP-SR-4	1.0E+01 - 2.2E+02
EFSFSR above Yellow Pine Pit	YP-SR-6	9.0E+00 - 2.2E+02
EFSFSR above Fiddle Creek	YP-SR-8	8.0E+00 - 2.0E+02
Lower Midnight Creek	YP-T-10	1.5E-01 - 3.3E+00
Lower Fiddle Creek	YP-T-11	4.5E-01 - 1.3E+01
Upper Fiddle Creek	YP-T-12	3.0E-01 - 1.9E+01
Scout Creek	YP-T-15	3.8E-02 - 9.8E-01
DMEA waste rock seep	YP-T-17	2.2E-03 - 3.3E-02
Rabbit Creek	YP-T-21	4.7E-02 - 3.2E+00
Garnet Creek	YP-T-35	6.7E-03 - 1.9E+00
Salt Creek	YP-T-40	1.0E+00 - 1.4E+01
Hennessy Creek	YP-T-41	1.9E-01 - 5.2E+00
Upper Midnight Creek	YP-T-42	2.9E-01 - 4.1E+00
Fern Creek	YP-T-44	2.0E-01
Spring feeding Fern Creek	YP-T-47	8.9E-03
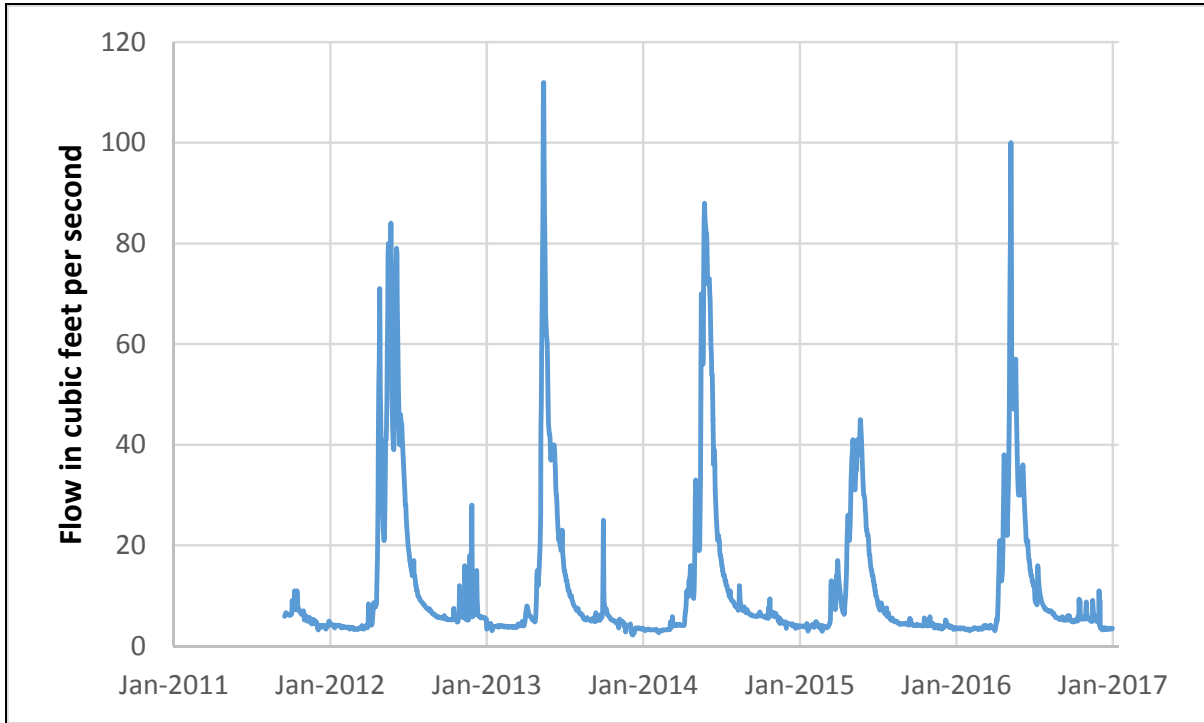
Figure 2.4. Flow in the EFSFSR above Meadow Creek, near Stibnite (USGS 13310800), linear scale.
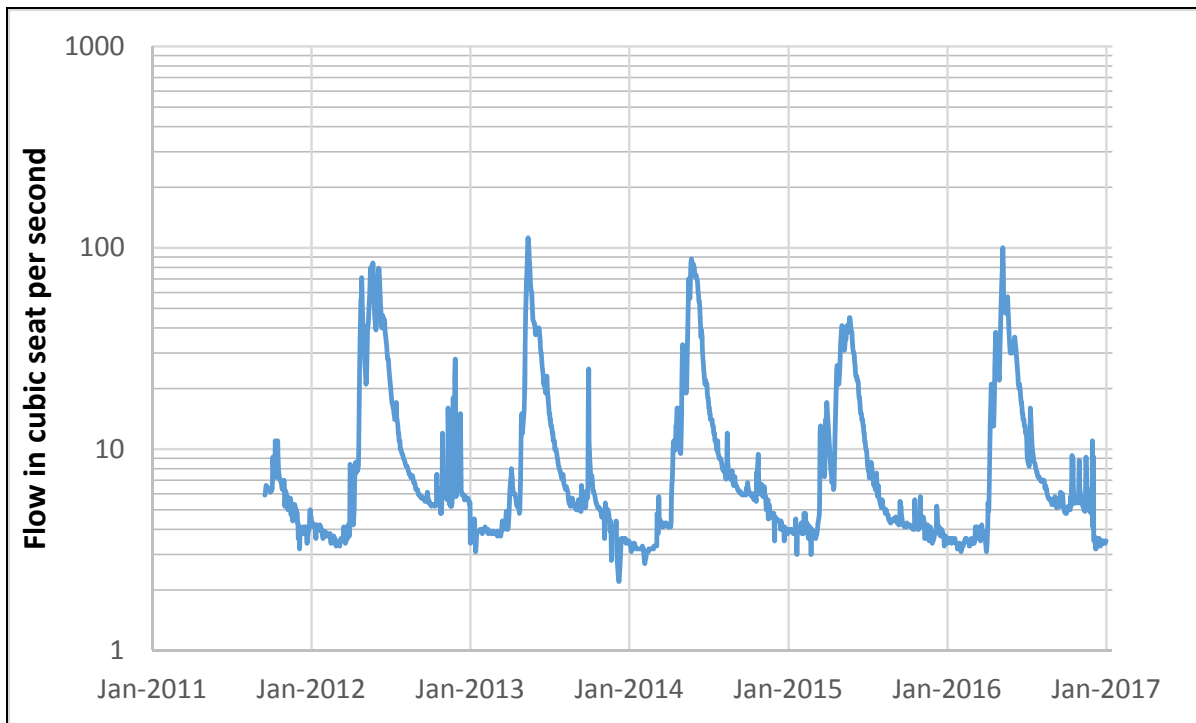
Figure 2.5. Flow in the EFSFSR above Meadow Creek, near Stibnite (USGS 13310800), log scale.
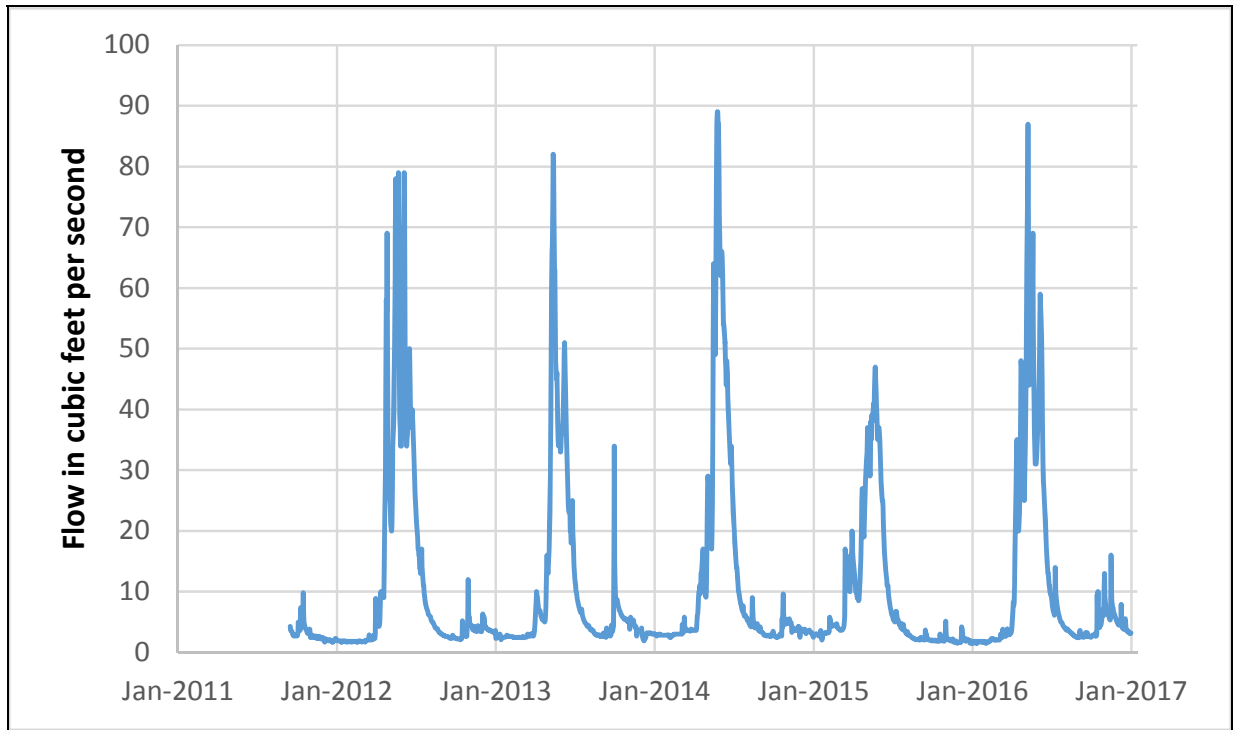
Figure 2.6. Flow in Meadow Creek near Stibnite (USGS 13310850), linear scale.
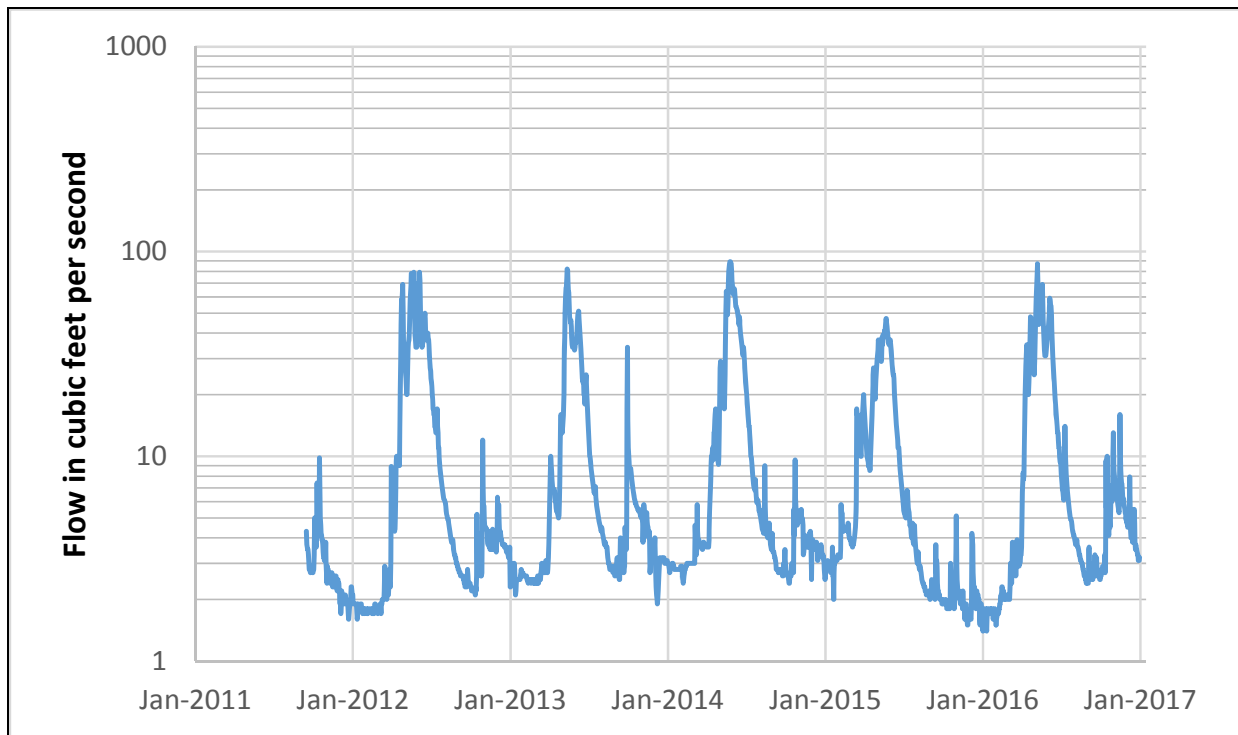
Figure 2.7. Flow in Meadow Creek near Stibnite (USGS 13310850), log scale.
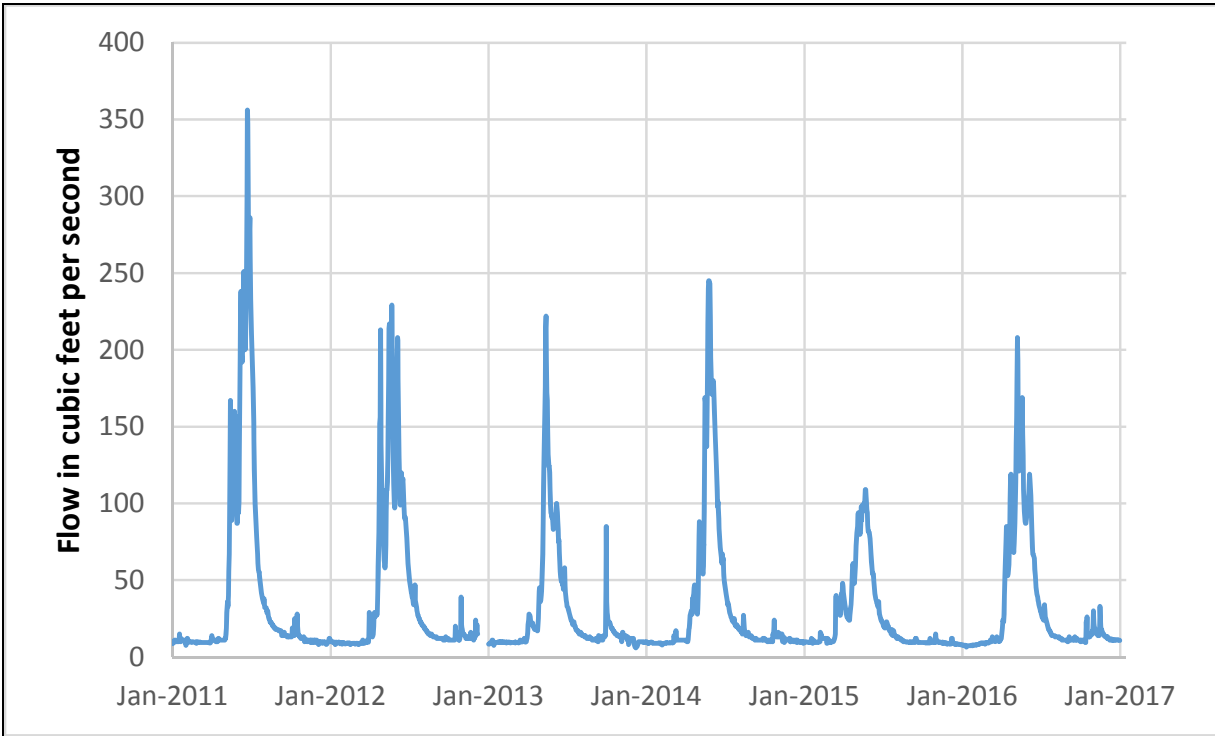
Figure 2.8. Flow in the EFSFSR at Stibnite (USGS 13311000), linear scale.
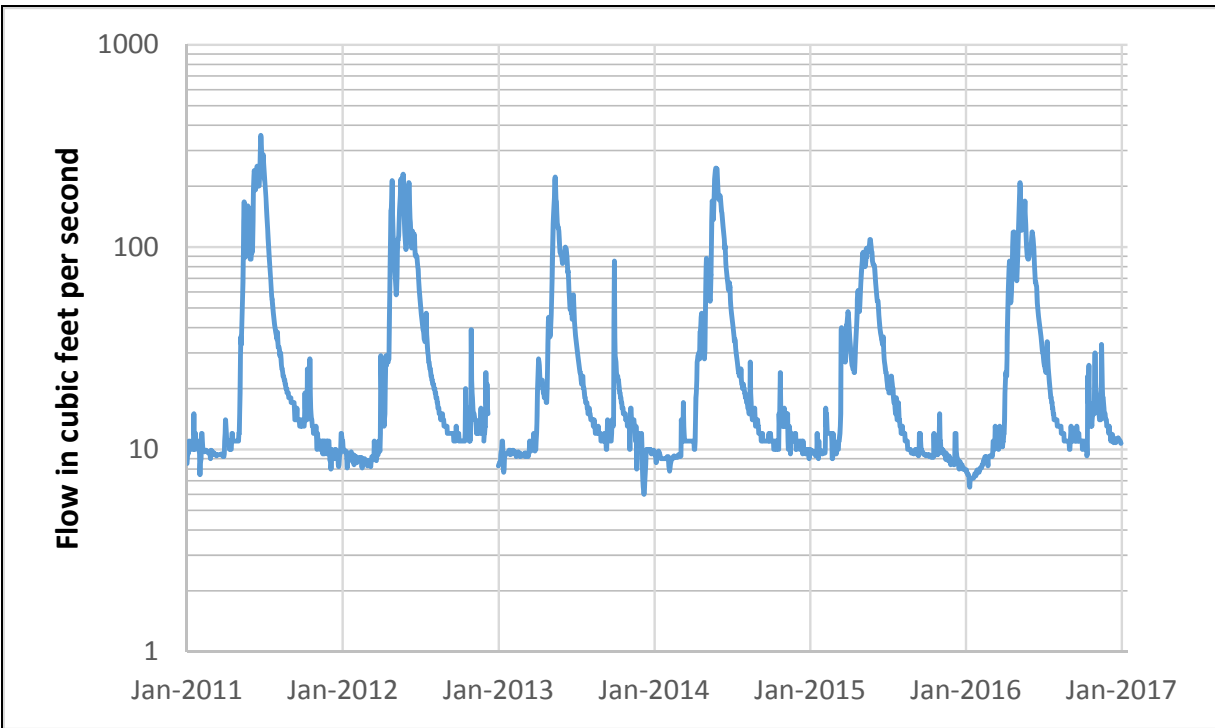
Figure 2.9. Flow in the EFSFSR at Stibnite (USGS 13311000), log scale.
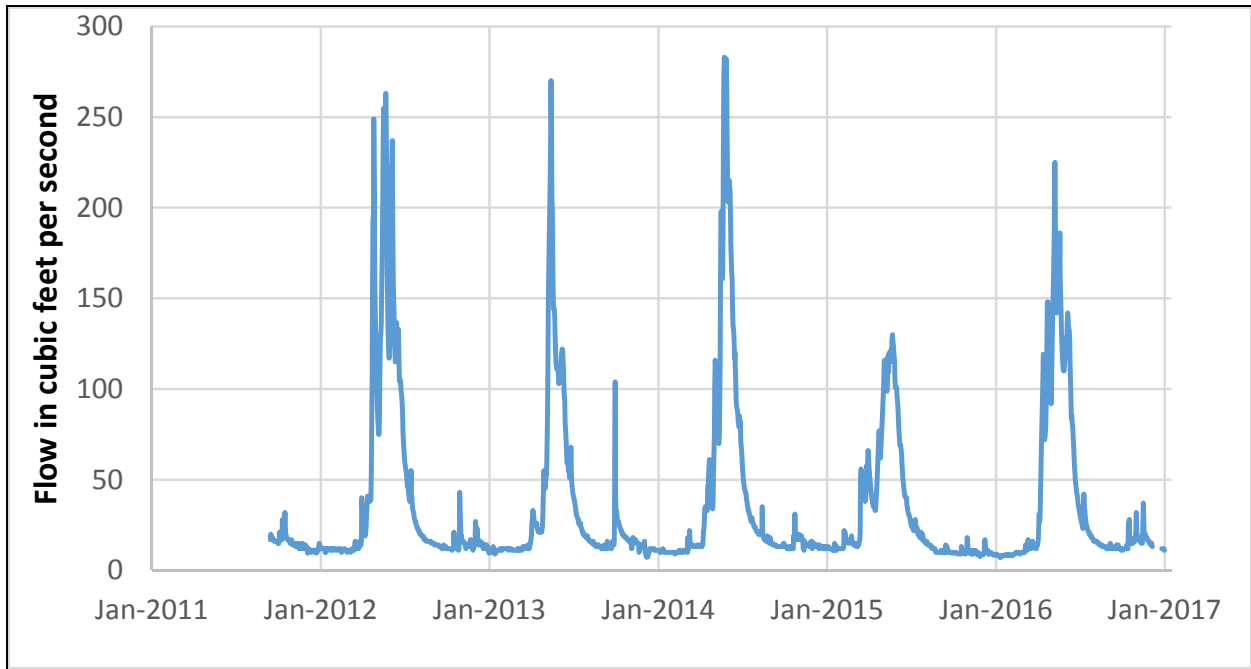
**Figure 2.10. Flow in the EFSFSR above Sugar Creek near
Stibnite (USGS 13311250), linear scale.**
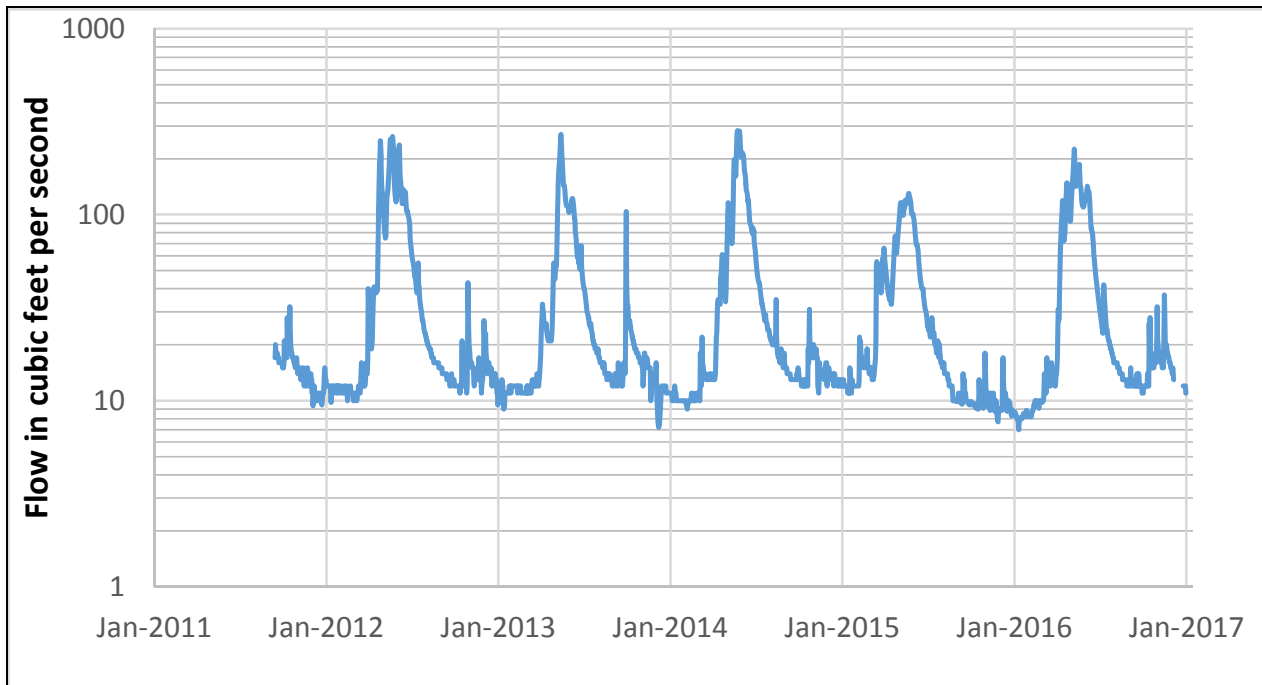
**Figure 2.11. Flow in the EFSFSR above Sugar Creek near
Stibnite (USGS 13311250), log scale.**
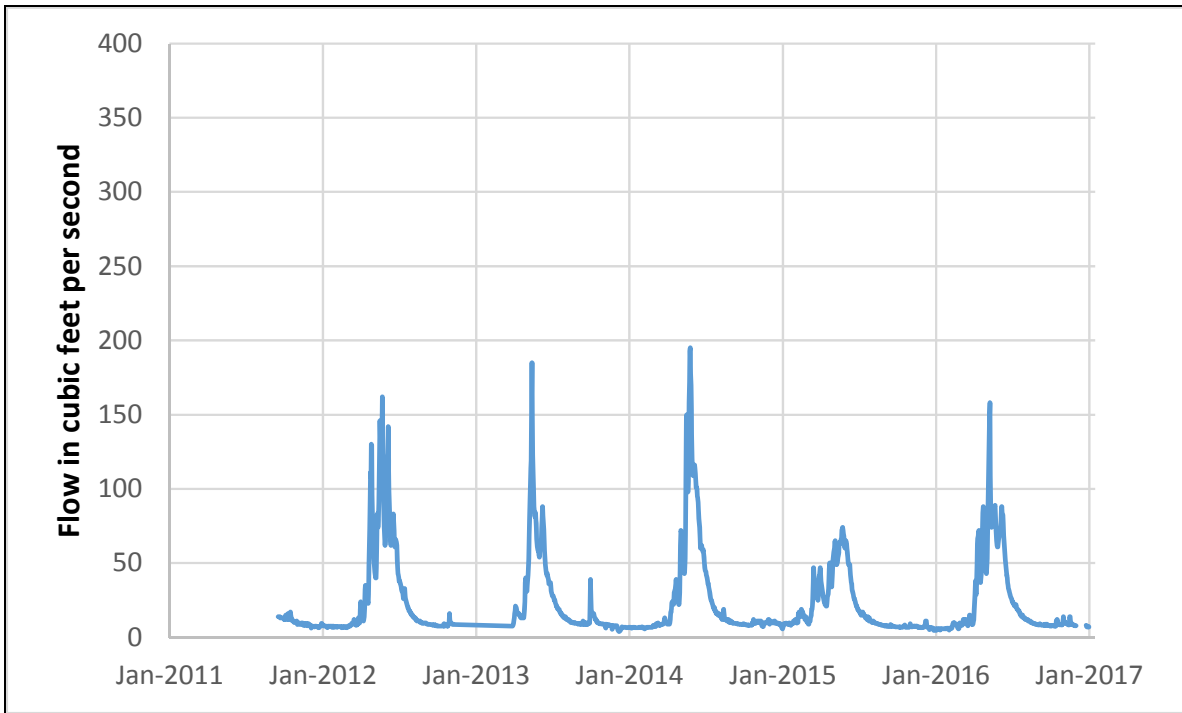
Figure 2.12. Flow in Sugar Creek near Stibnite (USGS 13311450), linear scale.
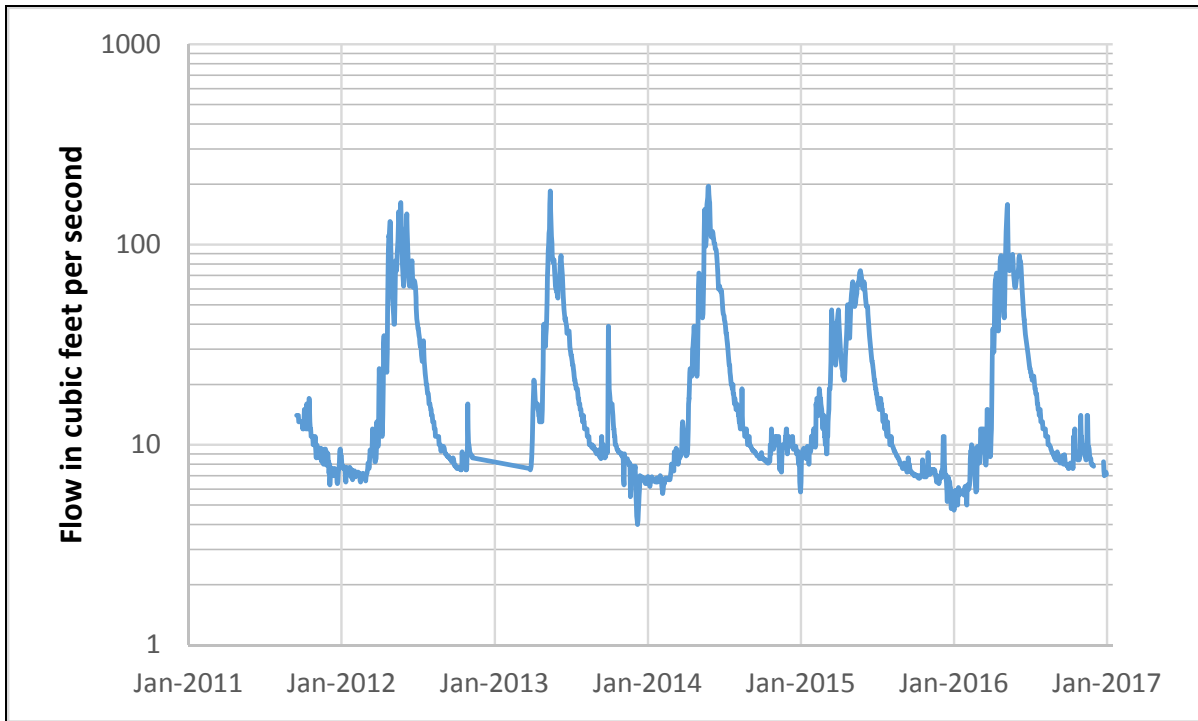
Figure 2.13. Flow in Sugar Creek near Stibnite (USGS 13311450), log scale.

2.2.3 Variability of Surface Water Flow

Among the USGS gages, the longest period of record is that for gage 13311000, EFSFSR at Stibnite, below the confluence with Meadow Creek. The gage has recorded daily streamflow for the periods 1928-1943, 1983-1997, and 2010-2016, with a cumulative total of 34 complete years of daily data, with the record shown graphically on Figure 2.14. The statistical distribution of daily flow at 13311000 is shown on Figure 2.15.
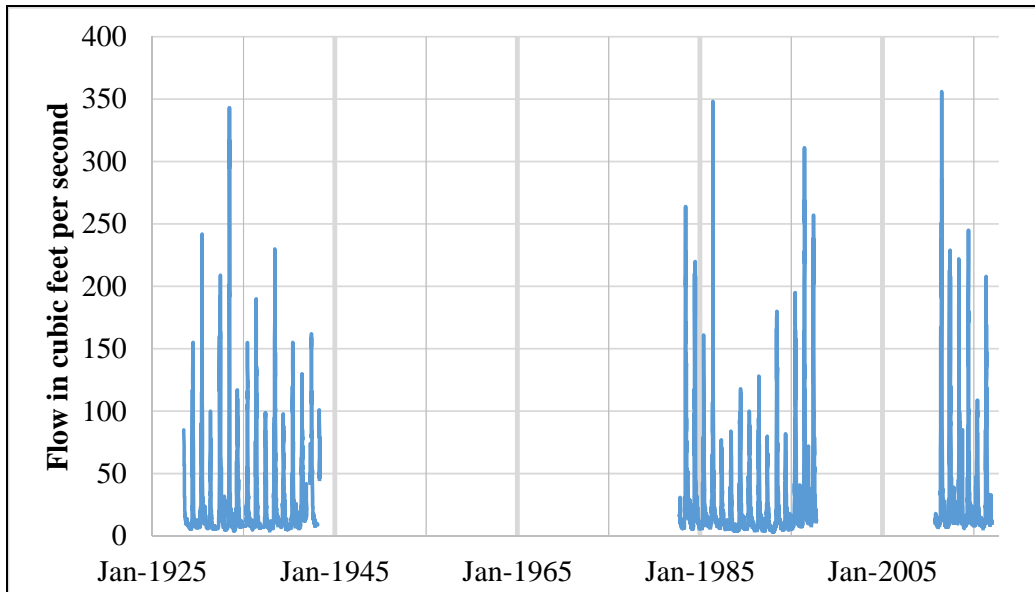
Figure 2.14. Flow in the EFSFSR at Stibnite (USGS 13311000).
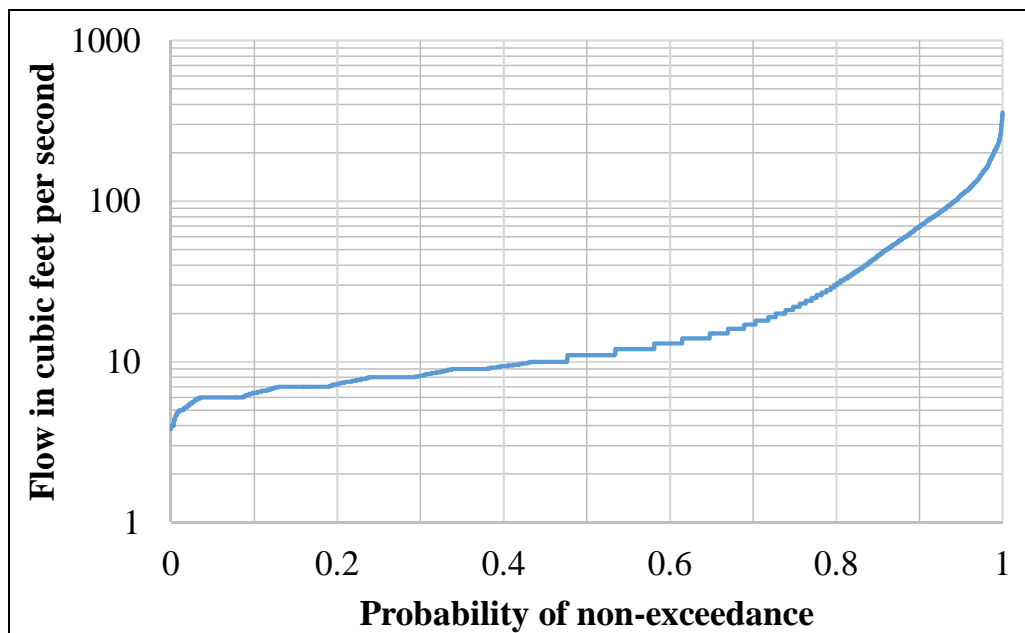
Figure 2.15. Distribution of daily flow in the EFSFSR at Stibnite (USGS 13311000).

2.3 Geology

The bedrock geology of the Stibnite area is defined by Late Cretaceous granitoids of the Idaho batholith and preserved roof pendants consisting of metasedimentary and metavolcanic units of the Proterozoic Windermere Group and Ordovician to Cambrian younger sedimentary units (Stewart et al., 2016). Unconsolidated units include glacial deposits and landslide deposits as well as fluvial deposits in the valleys. A geologic map (Geologic Resources Baseline Study, fig. 4-5; Midas Gold, 2017) is presented as Figure 2.16.

2.3.1 Bedrock Units

The Idaho Batholith is a Late Cretaceous two-stage intrusion consisting of a foliated older set of epidote-bearing hornblende-biotite tonalites preserved along the margin of the batholith and a younger, centrally located muscovite-biotite granite, granodiorite and quartz monzonite.

The more voluminous younger phase of the batholith forms most of the rocks in the Stibnite area and is thought to have intruded at a relatively shallow depth preserving stratigraphy, metamorphic gradients, and structures in the roof pendants (Stewart et al., 2016).

The Windermere Group consists of rift-related metamorphosed shallow marine, near-shore, volcanic, and terrestrial sedimentary rocks, including quartzite, biotite-aluminosilicate schist and phyllite, gray marble, calc-silicate gneiss, amphibolite, greywacke, and orthogneiss. Younger Paleozoic units are dominated by interbedded marbles and quartzites.

The Stibnite roof pendant is preserved along the east-side down Meadow Creek Fault, an area of rich mineral deposits. Neither batholith nor roof pendant rocks store or conduct appreciable amounts of water in the unfractured rock matrix. Water is transmitted locally in fractures, along faults and along contacts.

2.3.2 Unconsolidated Sediments

Glacial deposits include till and outwash, poorly sorted deposits that include cobbles, pebbles, sand, silt, and clay. Fluvial and alluvial deposits are generally better sorted silt, sand, pebbles, and cobbles, with generally physically mature clasts. Landslide deposits (colluvium) are present locally and consist of poorly-sorted silt- to boulder- sized material, generally characterized by a hummocky surface (Stewart et al., 2016).

2.3.3 Faults and Structures

A general west-northwest trend of the Neoproterozoic metasedimentary units was interpreted (Lund, 2004) to be related to a Neoproterozoic failed rift.
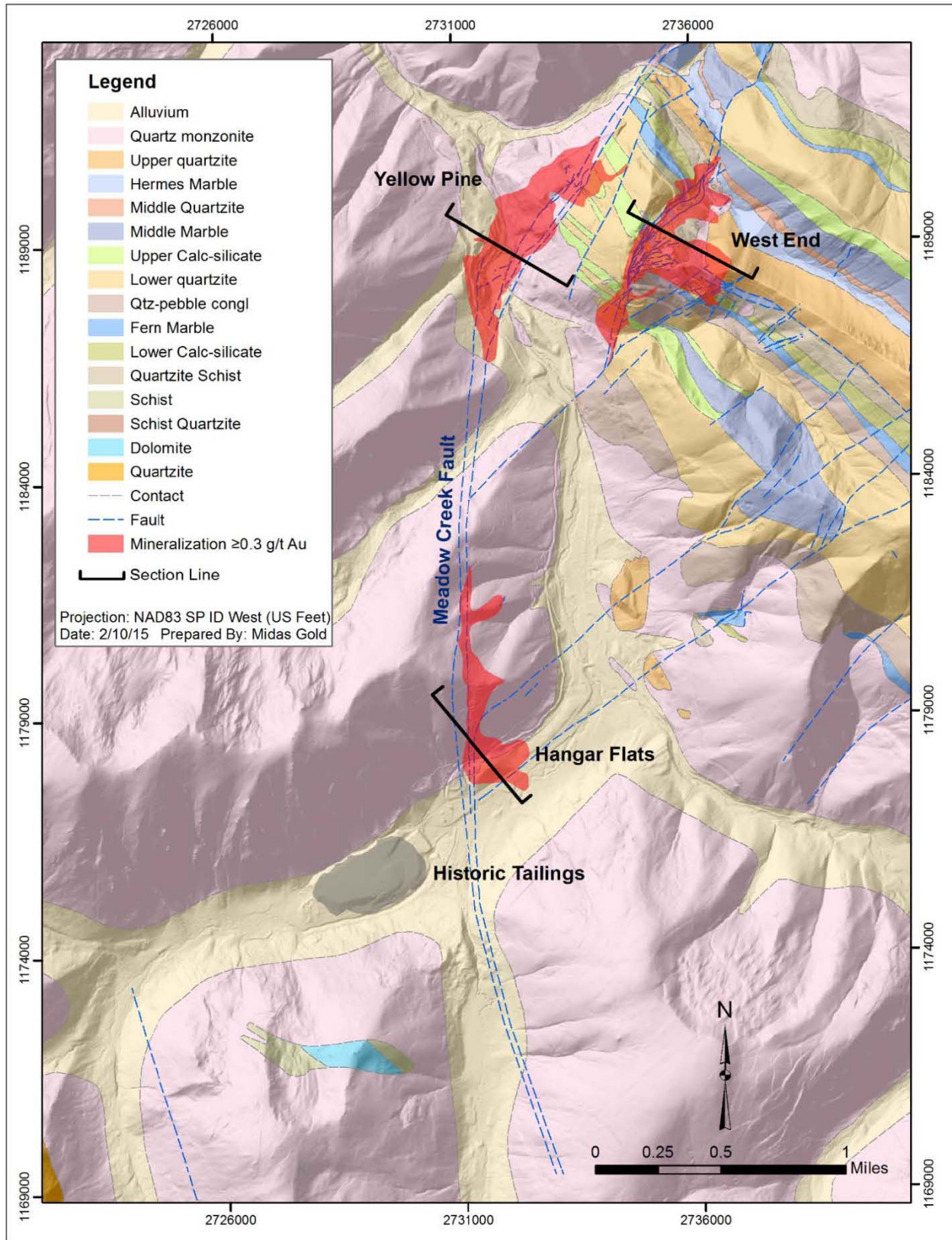
Figure 2.16. Stibnite District Geologic Map (Midas Gold, 2017, fig. 4-5).

The younger Meadow Creek Fault parallels the Johnson Creek-Profile Gap shear zone about 7 miles west of Stibnite, oriented about N 10 E. Both are down-thrown to the east, with higher metamorphic grades exposed to the west. The structural fabric represents a possible continuation of right-lateral transpression associated with structural readjustments after Idaho batholith intrusion and island arc collision (Lund, 2004).

Precious metal quartz-vein deposits in the Stibnite area are present within the Johnson Creek-Profile Gap shear zone as well as in the Meadow Creek Fault area, trending parallel to both. They are disrupted by Eocene brittle (normal) faulting characterized by north-northeast-trending fractures also associated with shallow Eocene plutons and extrusive volcanic rocks.

Groundwater flow and seeps and springs are found along the identified faults and structures, particularly where they cross the valley bottoms. All faults potentially may act as local conduits or barriers to groundwater flow. No evidence of groundwater movement in faults over long distances, or between basins, has been found.

2.4 Groundwater Hydrogeology

Groundwater flows along the main river valleys, in pockets of alluvium and in fractured bedrock. Away from the valley bottoms the bedrock of the mountain block is mainly impermeable and does not contain appreciable amounts of water.

2.4.1 Groundwater Occurrence and Flow System boundaries

Midas Gold has measured groundwater levels at monitoring points in the study area since November 2011. Locations of groundwater-level measurements are shown on Figure 2.17, and well details are listed in Table 2.5.

Some of the monitoring wells drilled, as well as Midas Gold exploration drill holes, penetrated essentially impermeable rock without encountering groundwater. The approximate extent of the groundwater system along the EFSFSR and tributaries is shown in a contour map of the local potentiometric surface presented on Figure 2.18.

The contours apply to all seasons and time periods, as the seasonal variability of groundwater levels, at less than +/- 10 ft (BC, 2017), is small compared to the relief shown on the study-area scale map.

2.4.2 Recharge and Discharge

Snow melt percolates down steep mountain slopes on the surface, in the overburden and in bedrock fractures, eventually recharging the groundwater systems along the stream channels. Groundwater then flows along and towards the EFSFSR and tributaries, eventually discharging to the stream system.
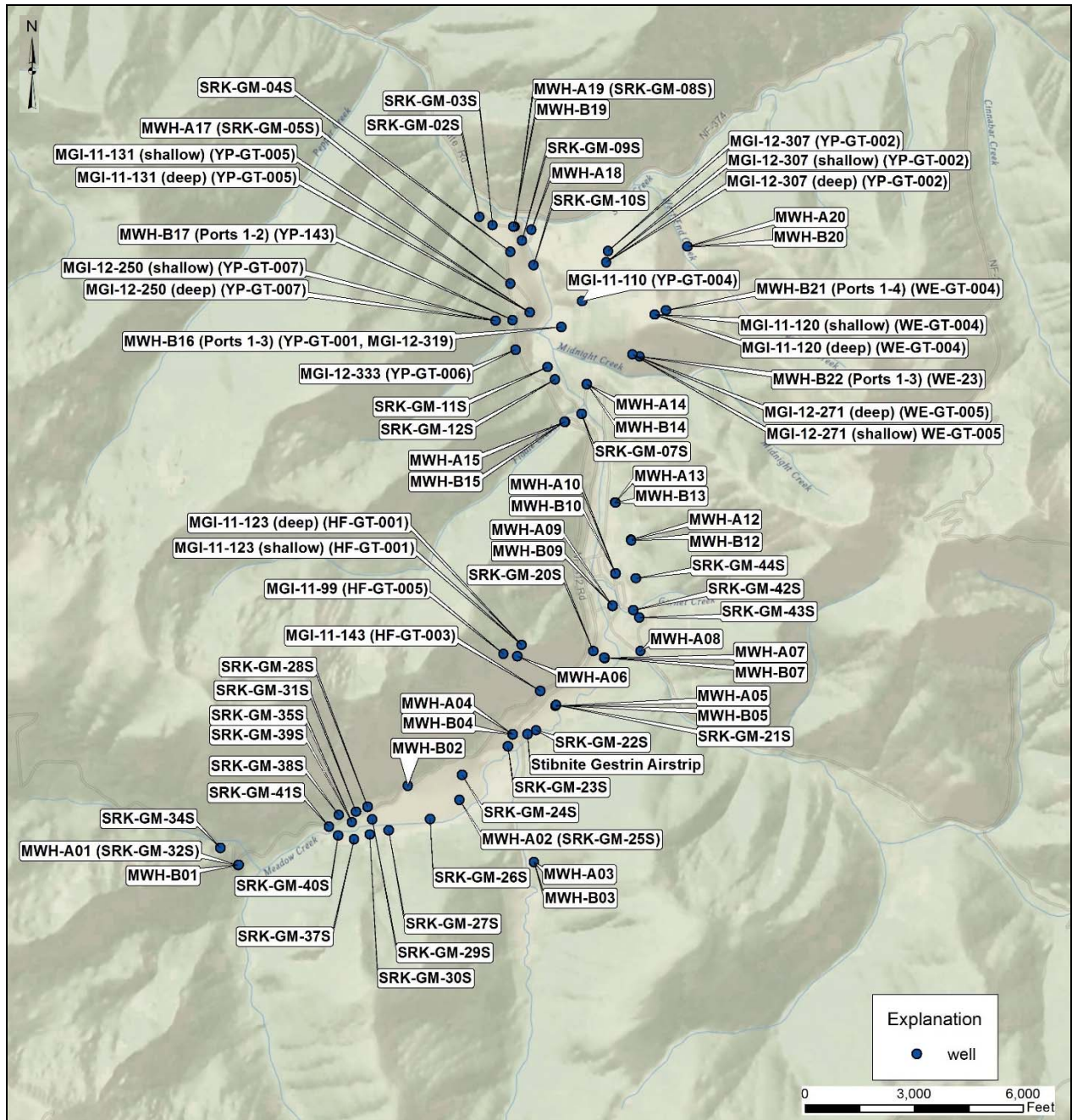
Figure 2.17. Groundwater monitoring locations.

Table 2.5. Groundwater monitoring points

well or borehole ID	elevation, ft amsl	X, ft, State Plane	Y, ft, State Plane	screen interval, ft
MWH-B21 (Port 1)	7,231	2074865	16326664	125 to 160 [a]
MWH-B21 (Port 2)	7,231	2074865	16326664	328 to 353 [a]
MWH-B21 (Port 3)	7,231	2074865	16326664	430 to 470 [a]
MWH-B21 (Port 4)	7,231	2074865	16326664	765 to 815 [a]
MGI-12-307	6,375	2073270	16328307	947 (TD)
MWH-B22 (Port 1)	6,969	2074143	16325387	91 to 121.5 [a]
MWH-B22 (Port 2)	6,969	2074143	16325387	228.5 to 389 [a]
MWH-B22 (Port 3)	6,969	2074143	16325387	400 to 536 [a]
MWH-B16 (Port 1)	6,157	2071981	16326211	166 to 222 [a]
MWH-B16 (Port 2)	6,157	2071981	16326211	451 to 476 [a]
MWH-B16 (Port 3)	6,157	2071981	16326211	567 to 618 [a]
MGI-12-333	6,316	2070724	16325578	-
MWH-B17 (Port 1)	6,307	2070639	16326395	116 to 177 [a]
MWH-B17 (Port 2)	6,307	2070639	16326395	394 to 425 [a]
MWH-A01	6,784	2063096	16311329	30 to 40
MWH-A02	6,660	2069179	16313137	100 to 110
MWH-A03	7,038	2071236	16311418	290 to 310
MWH-A04	6,564	2070639	16314944	55 to 64
MWH-A05	6,554	2071823	16315729	34 to 44
MWH-A06	7,326	2070770	16317110	9 to 14
MWH-A07	6,513	2073168	16317057	32 to 42
MWH-A08	6,526	2074163	16317248	28 to 38
MWH-A09	6,463	2073395	16318491	21 to 26
MWH-A10	6,392	2073477	16319390	20 to 30
MWH-A12	6,499	2073907	16320322	50 to 60
MWH-A13	6,428	2073467	16321358	50 to 65
MWH-A14	6,288	2072686	16324623	59 to 69
MWH-A15	6,364	2072089	16323586	70 to 75
MWH-A17	6,202	2070580	16327408	98 to 108
MWH-A18	5,927	2070705	16328977	20 to 30
MWH-A19	6,021	2075455	16328429	50 to 60
MWH-A20	6,650	2063100	16311335	43 to 53
MWH-B01	6,784	2067758	16313530	125 to 135
MWH-B02	6,635	2071229	16311414	48 to 58
MWH-B03	7,038	2070649	16314944	463 to 478
MWH-B04	6,564	2071836	16315748	238 to 258
MWH-B05	6,554	2073165	16317070	208 to 218
MWH-B07	6,513	2073395	16318504	284 to 294
MWH-B09	6,463	2073474	16319393	85 to 100
MWH-B10	6,392	2073910	16320309	78 to 88
MWH-B12	6,499	2073470	16321349	130 to 140
MWH-B13	6,428	2072689	16324629	120 to 130
MWH-B14	6,288	2072076	16323583	180 to 190
MWH-B15	6,364	2070665	16328977	154 to 184
MWH-B19	6,020	2075455	16328429	300 (TD)

a Sand pack interval (information on top of screen interval not provided).   d Recorded
b Depth calculated based on drilled length and borehole inclination.   amsl - above mean sea level
c Recorded daily.   TD - total depth

Table 2.5. Groundwater monitoring points (concluded)

well or borehole ID	elevation, ft amsl	X, ft, State Plane	Y, ft, State Plane	screen interval, ft
MWH-B20	6,650	2069733	16329242	385 (TD)
SRK-GM-02S	6,033	2070091	16329016	162 to 172
SRK-GM-03S	6,003	2070586	16328288	110 to 120
SRK-GM-04S	6,097	2072542	16323803	100 to 110
SRK-GM-07S	6,437	2070905	16328593	25 to 35
SRK-GM-09S	5,984	2071220	16327914	58 to 68
SRK-GM-10S	6,033	2071603	16325092	27 to 37
SRK-GM-11S	6,132	2071810	16324761	25 to 55
SRK-GM-12S	6,157	2072860	16317241	26 to 36
SRK-GM-20S	6,520	2071843	16315751	60 (TD)
SRK-GM-21S	6,495	2071289	16315059	170 to 180
SRK-GM-22S	6,549	2070518	16314620	149 to 159
SRK-GM-23S	6,521	2069248	16313826	88 to 98
SRK-GM-24S	6,582	2068372	16312608	107 to 117
SRK-GM-26S	6,572	2067230	16312300	74 to 84
SRK-GM-27S	6,562	2066649	16312950	55 to 65
SRK-GM-28S	6,615	2066787	16312599	27 to 37
SRK-GM-29S	6,553	2066715	16312172	38 to 48
SRK-GM-30S	6,581	2066328	16312805	47 to 57
SRK-GM-31S	6,569	2062598	16311808	34 to 44
SRK-GM-34S	6,901	2066226	16312513	29 to 39
SRK-GM-35S	6,613	2066282	16312047	39 to 49
SRK-GM-37S	6,631	2065865	16312713	21 to 31
SRK-GM-38S	6,591	2066226	16312520	44 to 54
SRK-GM-39S	6,564	2065839	16312146	44 to 54
SRK-GM-40S	6,632	2065596	16312395	28 to 38
SRK-GM-41S	6,582	2073962	16318373	45 to 55
SRK-GM-42S	6,503	2074130	16318179	27 to 37
SRK-GM-43S	6,487	2074035	16319255	25 to 35
SRK-GM-44S	6,640	2073943	16325446	12 (TD)
MGI-12-271 (shallow)	6,975	2073943	16325446	174 [b]
MGI-12-271 (deep)	6,975	2070173	16326378	382 [b]
MGI-12-250 (shallow)	6,512	2070173	16326378	402 [b]
MGI-12-250 (deep)	6,512	2071111	16326611	647 [b]
MGI-11-131 (shallow)	6,174	2071111	16326611	-
MGI-11-131 (deep)	6,174	2070892	16317412	704 [b]
MGI-11-123 (shallow)	7,431	2070892	16317412	397 [b]
MGI-11-123 (deep)	7,431	2073221	16327999	-
MGI-12-307 (shallow)	6,581	2073221	16327999	152 [b]
MGI-12-307 (deep)	6,581	2074556	16326549	294 [b]
MGI-11-120 (shallow)	7,270	2074556	16326549	215 [b]
MGI-11-120 (deep)	7,270	2070393	16317166	403 [b]
MGI-11-99	7,484	2071407	16316142	1,584 [b]
MGI-11-143	6,611	2072555	16326919	994 [b]
MGI-11-110	6,526	2071790	16315548	969 [b]
Stibnite Gestrin Airstrip	6,542	2074865	16326664	

a Sand pack interval (information on top of screen interval not provided).   d Recorded.
b Depth calculated based on drilled length and borehole inclination.   amsl - above mean sea level
c Recorded daily.   TD - total depth
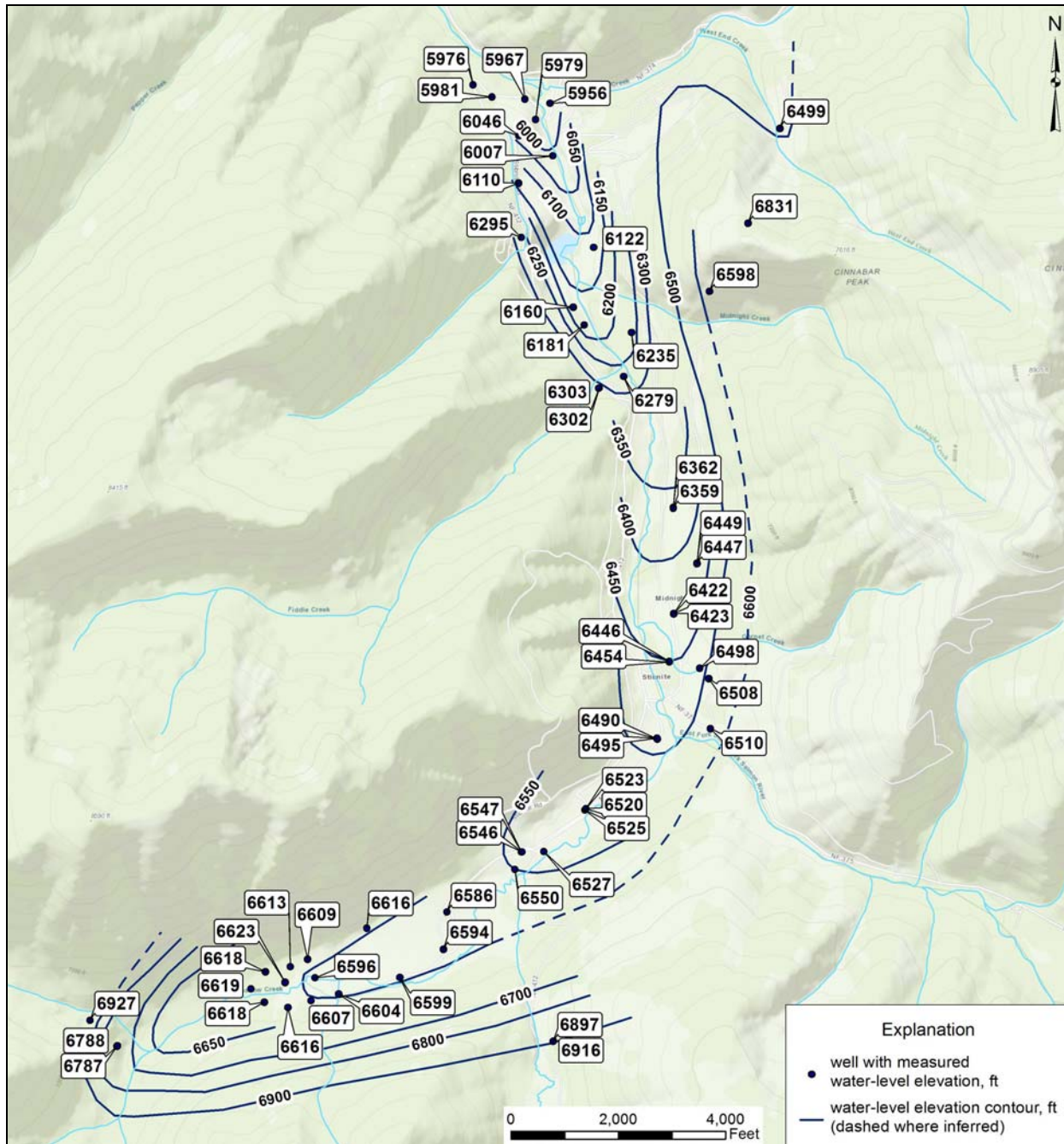
Figure 2.18. Groundwater level contours in the study area.

2.4.3 Groundwater Flow in Alluvium

A map showing the thickness of the soil, collegial and alluvial overburden prepared by Midas Gold is presented on Figure 2.19. The greatest thicknesses of alluvium lie along the valley bottoms, with a contiguous large thickness in Meadow Creek Valley that forms a significant alluvial aquifer.
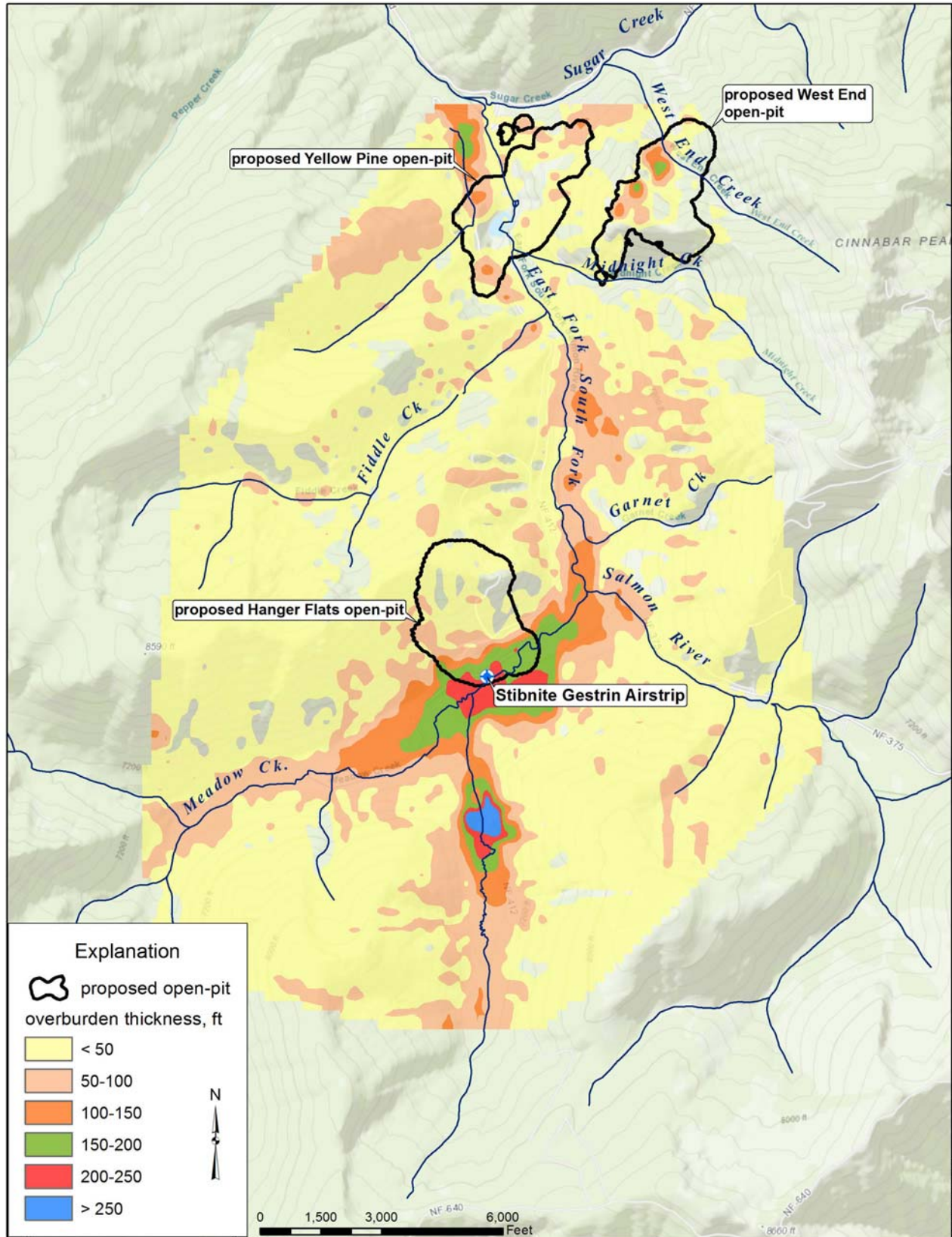
Figure 2.19. Thickness of overburden.

Pumping tests were performed at the Stibnite Gestrin Airstrip Well, completed in the Meadow Creek alluvium, in 1989, in February 2012, and December 2013. Results are presented in the WRSR (BC, 2017), revealing a permeable alluvial unit in close connection with Meadow Creek. An estimate of transmissivity of the alluvial aquifer from the pumping test was 3069 ft^2/day, corresponding to an estimated hydraulic conductivity of 10.2 ft/day (BC, 2017).

Other, smaller thicknesses of alluvium along the EFSFSR and its tributaries also contain groundwater. Groundwater levels are generally close to the nearby stream channel elevations. Hydraulic conductivity estimates for the alluvium developed from 21 slug tests (BC, 2017) range from 0.3 to 139 ft/day, with a geometric mean of 7 ft/day.

On the slopes above the valley bottoms there is a variable thickness of soil and colluvium over most of the area. This variably-saturated layer also conducts water and absorbs snowmelt that gradually drains to the groundwater system and the stream channels.

2.4.4 Groundwater Flow in Bedrock

Groundwater also flows in fractured bedrock along the axes of the main surface drainages and along individual faults or geologic contacts.

Responses in bedrock observation wells, to pumping of the Gestrin well, reveal a bedrock system distinct from the alluvium. But the response also indicates that the bedrock system is a compartment of limited extent, closely linked to the pumping well and to Meadow Creek. An estimate of transmissivity of the local bedrock feature (BC, 2017) was 1,345 ft^2/day.

Local Hydraulic conductivity estimates from 13 bedrock slug tests (BC, 2017) range from 0.03 to 4.9 ft/d, with a geometric mean of 0.4 ft/day. However, drilling in the non-fractured rock mass suggests it does not contain or conduct appreciable amounts of water.

The lack of an extensive bedrock aquifer was confirmed by a series of pressure-injection tests (SRK, 2012). Estimated hydraulic conductivities from the tests ranged from zero to 5.9 ft/day. Results show limited and sporadic permeability in bedrock, generally decreasing with depth, with no indication of systematic permeability or of an extensive flow system.

In summary, no extensive bedrock groundwater flow system has been found. Groundwater is locally contained in fractured bedrock along the valley bottoms and along faults, in isolated compartments or in connection with overlying alluvial systems. The bedrock does not form a distinct lower aquifer.

2.4.5 Regional Groundwater Flow

Neither the piezometer drilling program nor the Midas Gold exploration drilling program has identified any systematically permeable bedrock formations yielding substantial quantities of water or forming a distinct aquifer unit.

The lack of permeability in the primary rock mass results in groundwater flow that is local and compartmentalized. Most flow occurs close to and along the stream channels, within isolated alluvial pockets separated by bedrock constrictions. There is no regional groundwater flow system.

As a result, groundwater effects of the Project will be local. Any downstream or regional hydrologic effects will be limited to changes in flow and water quality in the EFSFSR

2.5 Water Balance

The long-term, regional-scale precipitation pattern from the PRISM model (Fig. 2.1) was scaled to match measured surface water discharge from the study area, to estimate the local elevation-weighted average precipitation and the basin water balance.

Figure 2.20 shows the statistical distribution of annual average flow at gage 13311000, divided by the 19.3 mi^2 watershed area upstream of the gage, showing an average yield of about 19 in./yr. Also shown is streamflow plus potential evapotranspiration of 21 in./yr (Table 2.1).

Because precipitation on the watershed discharges as either surface flow or evapotranspiration, the two curves represent likely lower and upper bounds for the elevation-weighted annual precipitation over the basin; precipitation is greater than streamflow, and less than or equal to streamflow plus potential evapotranspiration.

Actual precipitation is expected to be much closer to the upper curve than the lower, given the heavily vegetated watershed. An initial estimate of mean annual elevation-weighted precipitation on the USGS 13311000 watershed is therefore about 40 in (19 in/yr average surface flow plus 21 in/yr estimated potential evapotranspiration).

Table 2.6 presents one possible distribution of mean annual precipitation as a function of elevation that roughly agrees with the PRISM results (Fig. 2.1) at the lowest elevation (6,500 to 7,000 ft amsl) and results in an elevation-weighted basin average of 40 in./yr.

While the estimated annual average precipitation shown on Table 2.6 is reasonable, simple precipitation-elevation relationships do not consider the wind redistribution of snow or the uneven patterns of sublimation and melt that govern the distribution of meteoric water within an area. As a result, estimates of precipitation on smaller parts of the study area are more uncertain than those for the larger, gaged sub-basins.
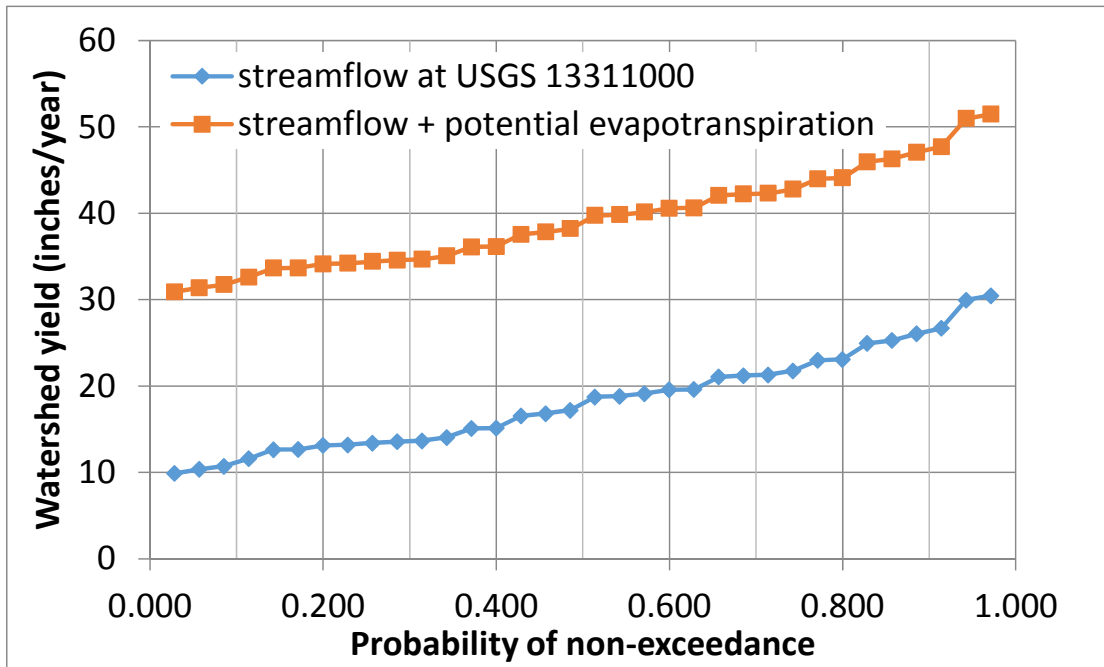
Figure 2.20. Streamflow per unit watershed area at USGS gage 13311000, and streamflow plus potential evapotranspiration.

Table 2.6. Sample precipitation-elevation relationship for the USGS gage 13311000 watershed

from elevation (ft amsl)	to elevation (ft amsl)	area (mi²)	mean annual precipitation (in.)
6,500	7,000	2.06	32
7,000	7,500	4.18	36
7,500	8,000	6.50	40
8,000	8,500	5.18	44
8,500	9,000	1.36	48
9,000	9,500	0.02	52
Total		**19.30**	
weighted average			40

ft amsl - feet above mean sea level

3.0 MODEL DEVELOPMENT

3.1 Model Structure and Software Used

The hydrologic model combines a spreadsheet-based (.XLS) meteoric water balance with a numerical model (MODFLOW) of groundwater and surface-water flow. The model computational structure is shown on Figure 3.1.
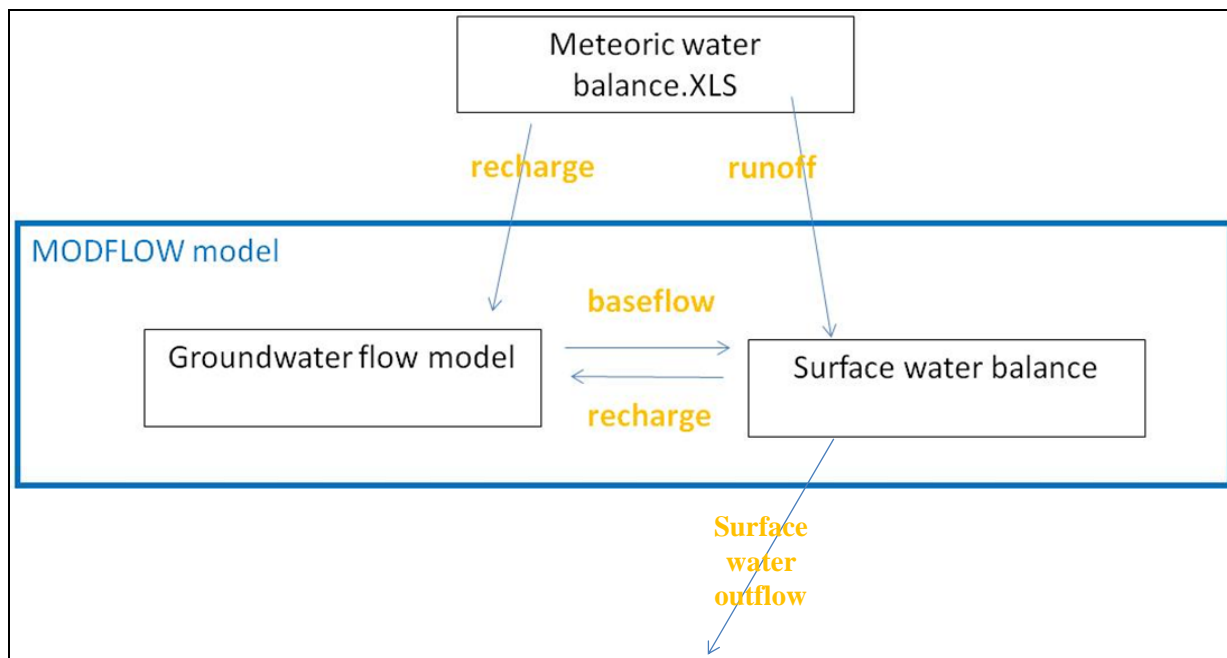
Figure 3.1. Model structure.

Monthly snowmelt and rainfall computed by the meteoric water balance are input to the numerical model as groundwater recharge and surface-water runoff. The numerical model computes monthly groundwater levels and surface-water flows throughout the model domain. The numerical model is developed using the USGS *Modular Three-Dimensional Finite Difference Ground-Water Flow Model, MODFLOW* (McDonald and Harbaugh, 1988).

The same approach has been used successfully to model other snowmelt-dominated mountain-block basins in Argentina (Jones, 2004; IDIH, 2006,), Chile (Jones, 2006) and British Columbia (JSAI, 2016).

The initial model is developed and calibrated using the JSAI in-house version of MODFLOW (JSAI, 2011). It is linked to the meteoric water balance by spreadsheet tools that generate MODFLOW input files from the meteoric water balance results. The JSAI code has been in use for over 20 years and has been thoroughly reviewed, tested, and documented. Program, source code and documentation are available for free from JSAI.

The model will also be implemented in a version using the USGS code MODFLOW-NWT (Niswonger, et. al, 2011), which is capable of simulating the same model and is supported by the popular software GroundWaterVistas (GroundWaterVistas does not support the link to the meteoric water balance). Like the JSAI code, MODFLOW-NWT preserves the mass balances of dry cells, a water-accounting detail important to simulations with model cells that dry and rewet, a feature used by this model.

Model files for the MODFLOW-NWT version will be provided in GroundWaterVistas format for review by the Agencies. The MODFLOW-NWT version will also be verified by generating all of the same outputs found in the modeling reports as well as the electronic outputs provided to other Site Models as illustrated on Figure 3.1.

Inputs to the model include (1) discretization of the model domain, (2) hydraulic parameters that control the flow of water within the model domain, and (3) boundary conditions that control the addition and removal of water to and from the model domain.

The meteoric water balance is described below, followed by descriptions of the preliminary numerical model discretization, aquifer parameters, and boundary conditions. All reported estimates of parameters to be used are provisional, pending model calibration.

3.2 Meteoric Water Balance

Inflows to the model from snowmelt and rainfall are computed using a spreadsheet-based monthly water balance that tracks precipitation as rain and/or snow, sublimation, snowpack accumulation, snowmelt and evaporation. The meteoric water balance is described by equation (3.1):

$$M_k = P_k + (S_{k-1} - S_k) - E_k \tag{3.1}$$

Where:

P_k = precipitation, month k

S_k = snowpack; $(S_{k-1} - S_k)$ is snowmelt for month k.

E_k = sublimation + evapotranspiration

M_k = snowmelt + rainfall.

M_k is the monthly water input to the numerical model. The numerical model in turn computes monthly groundwater and surface water balances.

Precipitation is estimated as described in Section 2.5 above using the 122-year monthly precipitation series from the PRISM model, scaled based on streamflow and potential evaporation data.

The maximum sublimation rate is initially assumed at 0.02 inches per day (0.5 mm/day, or 35 percent of annual potential evaporation, based on Jones, 2006 and JSAI, 2015). The actual monthly sublimation is computed as the maximum rate, limited to the available snowpack.

Snowmelt is estimated as a function of monthly average temperature, recorded at Stibnite from 2011. Melt is estimated as a function of temperature using the degree-day equation (3.2):

$$M_k = (S_{k-1} + P_k - E_k) * \min(1, \max(0, [t-t_f] / [t_m-t_f])) \tag{3.2}$$

Where:

$(S_{k-1} + P_k - E_k)$ in mm is the total water-equivalent snowpack available to melt,
t_m = "melting temperature" is the threshold temperature for complete melting,
t_f = "freezing temperature" is the threshold temperature for melt to stop,

So, for $t > t_m$, all available snow melts. For $t < t_f$, no melt occurs. For t between t_m and t_f, a portion of the snow melts in proportion to t. The melting and freezing temperatures were adjusted to match the observed timing of annual high flows.

Input to the numerical model was computed as rainfall plus snowmelt, minus evaporation. Evaporation was estimated as a linear function of available melt water and rainfall and on potential evaporation as a function of elevation. The computation of evaporation is as follows:

$$\text{evaporation} = \min (Q, \min(1, aQ+b)*PET)$$

Where:

Q = snowmelt + rainfall
PET = potential evaporation, computed from temperature, elevation, and latitude
a and b = empirical coefficients

The parameters of the water balance model are adjusted to match measured stream flows over the period 2011-2016. Preliminary meteoric water balance parameters are summarized on Table 3.1.

Table 3.1. Meteoric water balance parameters

parameter	value	unit
melting temperature t_m	12	(deg C)
freezing temperature t_f	2	(deg C)
evapotranspiration coefficient a	.0008	(inch/inch)
evapotranspiration coefficient b	0	(inch)

The 122-year scaled precipitation series is then applied to the calibrated water balance to derive a corresponding time series of monthly water inputs to the numerical groundwater model that are used in projections of future flows.

The monthly water input to the numerical model is divided into components of groundwater recharge and stream-flow runoff:

- All available water, up to a specified maximum, is input as groundwater recharge. The specified maximum recharge rate is set through model calibration to match measured winter base flows in surface streams.

- All water above the specified maximum recharge rate is input as surface water runoff.

3.3 Model Domain and Discretization

The following sections describe the preliminary horizontal (map view) discretization of the watershed forming the model domain, the approach to vertical discretization of the hydrogeologic system, and the approach to time discretization employed in model simulations.

3.3.1 Horizontal Discretization

The preliminary model grid consists of 224 rows, 145 columns, and 2 layers. Horizontal grid spacing ranges from 328 ft (100 m) at the edge of the model domain down to 30 ft in the vicinity of Hangar Flats open pit and the Meadow Creek alluvial aquifer to provide for finer discretization in the major area of groundwater flow, potential dewatering, and water-supply pumping.

3.3.2 Model Layering

The model will be developed using 3 vertical model layers. Layer 1 represents the overburden, with a thickness from the current ground surface as shown on Figure 3.2. The layer is unconfined. In the main valley bottoms, the overburden forms an aquifer that is recharged during the

annual melt and discharges water to the stream system year-round.

Above the valley bottoms the overburden does not form an aquifer, but it retains melt water in storage that slowly drains downhill to the groundwater and surface water system below. Cell rewetting is used to allow model cells representing overburden to seasonally become dry, then rewet during the annual melt.

Layers 2 and 3 represent the bedrock. Layer 2 represents shallow weathered bedrock with permeable zones directly beneath the valley bottoms, the approximate extent of which is shown on Figure 3.2. Most of the storage and flow of water occurs in the upper part of the bedrock, as fractures decrease with depth. Layer 3 represents low-permeability deep bedrock. Layers 2 and 3 comprise bedrock to a depth of 1,000 ft.

At this time, the need for more detailed layering of the model domain is not warranted. If model development or calibration should require, the model domain could be further discretized into multiple layers representing various depths of bedrock. The need for such modifications is not currently anticipated.

3.3.3 Time Discretization

Model simulations are provisionally based on a monthly time step interval. Several model simulations represent different time periods and conditions:

1. **Historical**: Representing the period 1895–2016. The PRISM-derived precipitation for this period is input to the model and simulated surface water flows and groundwater levels are compared to measured results from 2011-2016 to evaluate the model calibration.

2. **Future mining scenarios**: Simulating the effects and results of selected mining scenarios, including the no-mining scenario. Results include projected dewatering rates, surface-water diversion flows, groundwater-level changes, streamflow changes and water balance changes. The effects of each mining scenario are evaluated by comparing results to the equivalent results of the no-mining scenario.

3. **Future post-mining scenarios**: Simulating the post-mining period for each future scenario listed above, including the no-mining scenario. Results include recovery of groundwater levels, refilling of open pits, and effect of closure activities including covering and regrading of tailings and development rock storage facilities.
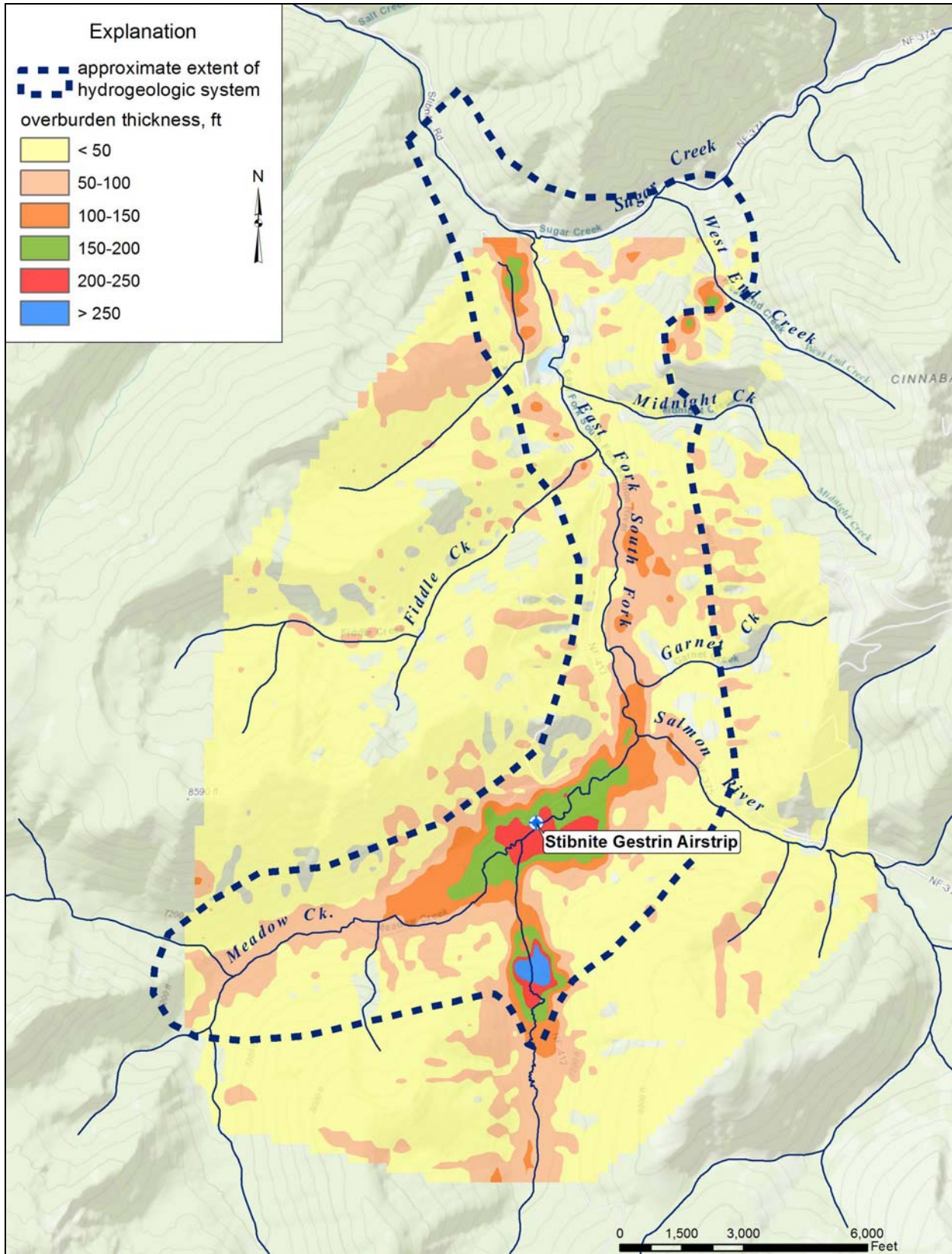
Figure 3.2. Overburden thickness.

No steady-state simulation is anticipated because the system is constantly in a seasonal flux and has no steady state. Instead, a seasonally-steady solution is obtained by running the 122-year transient simulation iteratively: The ending water levels from each iteration are used as the starting water levels for the next, until a long-term stable result is obtained.

For each of the future mining scenarios, climate variation will be assessed by, at a minimum, simulating dry, wet, and average climate sequences based on the long-term PRISM dataset. Changes to physical conditions during mining, such as development of the TSF, DRSFs, open pits, and stream routing will be assessed based on annual changes to facility configurations. Changes in simulated dewatering flow rates will be on an annual basis, but may be changed to monthly based on simulated output.

Output from the groundwater flow model will include (but is not limited to) the following;

- Regional and site-specific groundwater balances (flow rates), including inflows from recharge, throughflow, interactions with local surface water, changes in storage, etc.

- Groundwater/surface water interactions, including base flow from groundwater, surface seepage into groundwater, and accumulated surface flow volumes.

- Regional and site-specific groundwater levels, including changes in groundwater levels in response to operational activities and over the post closure period.

- Simulated groundwater fluxes specific to operational and closure activities, such as dewatering rates and inflow rates to open pits.

- These outputs will be presented in both tables and figures as appropriate. Maps showing the location of water withdrawals and inputs due to proposed operations will be provided, including diversions (ground and surface), discharges, injection wells, etc.

3.4 Hydraulic Parameterization

3.4.1 Aquifer Parameters

Aquifer parameters will be developed to appropriately represent the groundwater flow system. Parameterization will be kept as simple as possible:

- At a minimum, distinct hydraulic parameters will be assigned to zones in layer 1 representing (1) valley-bottom alluvium and (2) colluvial overburden.
- At a minimum, distinct hydraulic parameters will be assigned to layer 2 zones representing (1) the relatively fractured rock along the valley bottoms and (2) the relatively impermeable rock of the mountain block.

Additional detail and local variability will be added to the hydraulic parameterization if deemed necessary for development and calibration of the model. The model will include sensitivity analyses to assess the potential influences of more permeable faults and geologic structures on simulated groundwater flow and flow rates into the planned mine pits.

3.5 Boundary Conditions

Model boundary conditions include the categories of natural boundary conditions and anthropogenic boundary conditions. The natural boundary conditions, including (1) direct recharge and (2) stream-channel boundaries, are applied to all model simulations.

Model projections include different anthropogenic boundary conditions such as open-pit dewatering, post-mining open pits, water-supply pumping, surface water diversion and the effects of covers/liners.

Water consumed by evapotranspiration is accounted for in the meteoric water balance described above and is not directly simulated in the numerical model. Although evapotranspiration of groundwater occurs from the low-lying areas where groundwater is present, the same areas also receive substantial recharge from snowmelt and runoff, and also discharge water to the stream system. The accounting of evapotranspiration within the meteoric water balance is thus considered an appropriate simplification.

3.5.1 Groundwater Recharge

Direct groundwater recharge is represented as a specified-flow boundary condition using a direct recharge module for MODFLOW. Recharge is applied uniformly over the entire model domain during months with snowmelt or rainfall input, as computed by the meteoric water balance.

Recharge input is limited to a specified maximum rate, above which all excess water is input as surface-water runoff. The maximum recharge rate is calibrated to match model-simulated winter base flows with measured surface flows.

3.5.2 Surface Water Runoff and Stream-Groundwater Interaction

Runoff to stream channels, groundwater infiltration from stream channels, groundwater discharge to stream channels and surface-water outflow are represented using a streamflow-routing module for MODFLOW.

Stream cells are grouped into reaches to define the stream network; each reach defines a length of stream, with a specified downstream reach. A preliminary set of stream reaches to be simulated in the model are shown on Figure 3.3. Additional reaches will be added as required for model calibration and accurate representation of the flow field.
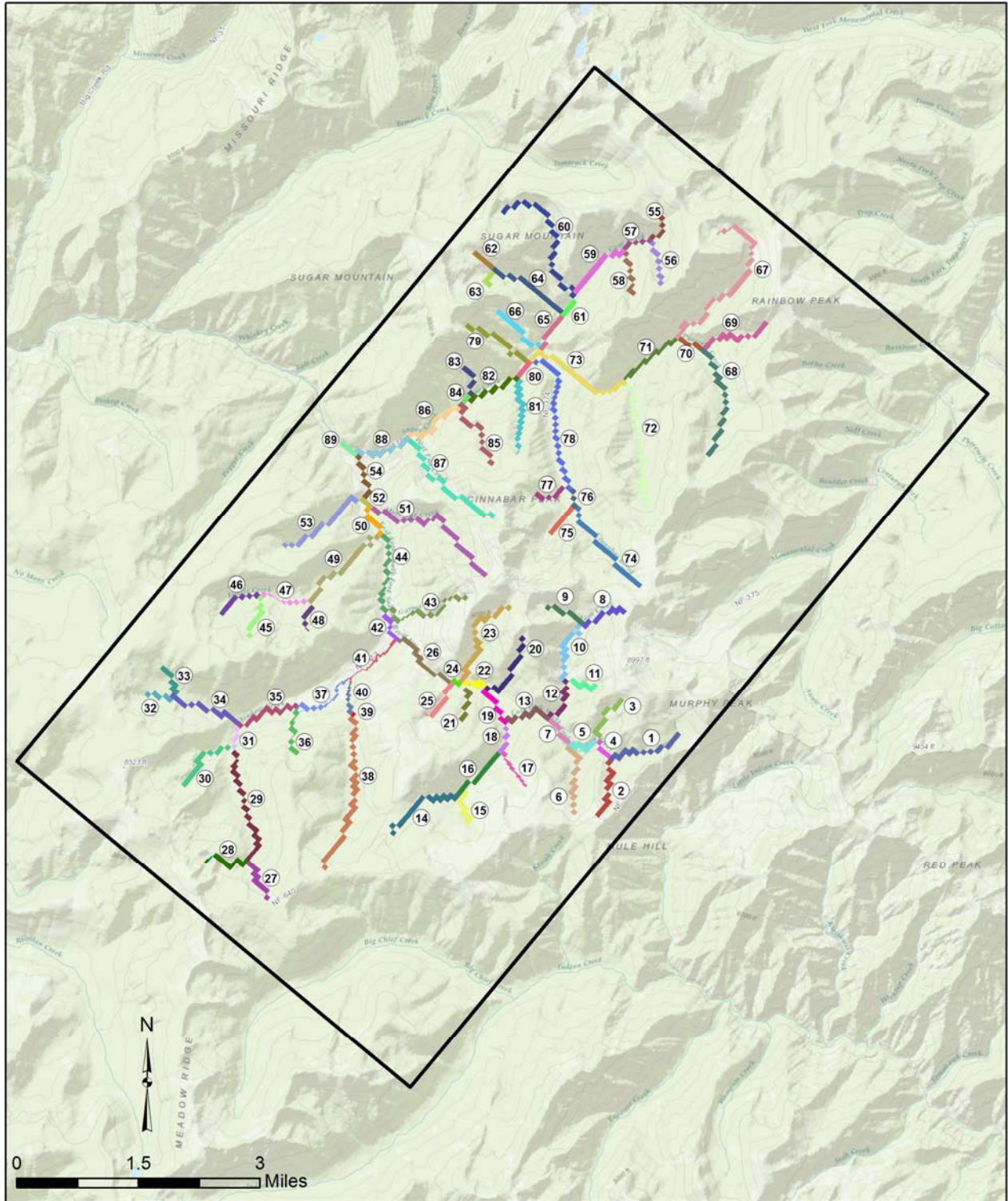
Figure 3.3. Simulated river reaches.

Runoff is added at the upstream end of each reach. For each cell within a reach, infiltration to groundwater or discharge from groundwater is computed, limiting infiltration to available streamflow. The computed infiltration or discharge is added or subtracted to the simulated streamflow, and the resulting total flow, if any, is passed to the next cell downstream.

Stream cell parameters include water stage elevation and conductance:

- Stream stage elevation for each cell is estimated from the stream bed topographic elevation. As a starting estimate, stream stages are fixed at a constant elevation; the observed time-variability of stream stage is insignificant compared to the spatial range of stream bed elevation found within each model cell.

- Conductance is based on model calibration. As a starting estimate, stream conductances are fixed, as the steep topography limits any seasonal changes in stream-channel geometry that would significantly alter streambed conductance.

Flow between stream cells and the corresponding aquifer model cell is computed based on river cell conductance, multiplied by either (1) the stream stage-aquifer head difference (aquifer in contact with stream bed) or (2) the stream stage-streambed bottom difference (aquifer below stream bed). Infiltration to the aquifer is further limited to the amount of simulated flow available in the stream.

3.5.3 Anthropogenic Boundary Conditions

Model projections will simulate different anthropogenic conditions for different simulations and time periods, including:

- Pumping from wells (specified-flow boundaries), for active dewatering ahead of mining and for providing water supply

- Passive flow to operating open pits (drain boundary conditions)

- Surface water diversions (changes to stream boundary conditions)

- Effects of covers/liners (no-flow boundaries or changes to recharge boundary conditions)

- Post-mining open pits (changes to stream boundary conditions)

Specific changes to the model to support simulation of proposed actions during mining may include (but is not limited to) the following:

- The tailings facility liner will be treated as a barrier to flow at the surface; recharge rates will be set to zero (for purposes of water-quality evaluations recharge may also be set to a small rate representing the statistical occurrence of potential liner leaks.).

- The lined Meadow Creek diversion will be treated as a leaky barrier to flow; the sensitivity of results to a likely range of channel leakage rates will be evaluated. The proposed-condition model will evaluate the effects of lined channel on groundwater recharge, storage, and baseflow discharge.

- As a barrier at the land surface, the presence of a liner has no implications for model layering. However, the number of layers may increase, in order to simulate dewatering of bedrock and a decrease in inflows to the open pits over time.

3.5.4 No-Flow Boundaries

No boundary conditions (no-flow boundaries) are specified for the horizontal and bottom perimeters of the model domain, reflecting the lack of a regional groundwater system. All study area groundwater that is not consumed by local evapotranspiration will then discharge to the EFSFSR.

4.0 MODEL CALIBRATION

4.1 Calibration Approach

The steps to calibrate the model are:

1. Adjust parameters of the meteoric water balance to obtain approximately correct timing and magnitude of annual high surface flows.

2. Adjust maximum recharge rate (possibly with additional adjustment to meteoric water balance parameters) to match overall magnitude of winter low flows.

3. Adjust aquifer and stream parameters (and possibly recharge rate) to match the recession of baseflows from the annual melt to the following year.

4. Adjust aquifer and stream parameters to match the overall pattern of groundwater levels throughout the study area.

5. Adjust storage parameters to match the observed seasonal fluctuation in water-level hydrographs (BC, 2017).

6. Adjust local (or global) aquifer parameters, using a simulation of the December 2013 pumping of the Gestrin airstrip well (BC, 2017), to match aquifer test results.

7. Adjust local (or global) aquifer parameters, using a simulation of the dewatering of the existing Yellow Pine pit, to match the low historical dewatering flows.

Calibration will be based on manual adjustments to the parameters described above. Use of automated calibration techniques is not planned at this time, but automated techniques could be applied if found to be helpful.

Standard model statistics will be reviewed to assess model calibration, including (but not limited to) average and absolute residuals, root-mean squared error (RMSE), and the ratio of the RMSE to the range of measure heads. Graphs and maps illustrating model calibration will be provided.

4.2 Surface Water Flows

Parameters of the meteoric water balance will be adjusted to match the timing and approximate magnitude of the annual high flows. Recharge rates and aquifer parameters will be adjusted to match the magnitude of winter low baseflows and the timing of the transition between high and low flow periods.

However, a year-by-year match between measured and simulated annual high flows is not expected. This is illustrated on Figure 4.1 comparing the precipitation input from the PRISM model with the measured water-year average flows at USGS 13311000, EFSFSR at Stibnite.

The correlations for the period of record and for the model calibration period of 2011-2016 are limited. The model will be calibrated to match the range and distribution of the annual high flows, but will not expect to match the flow for each year.
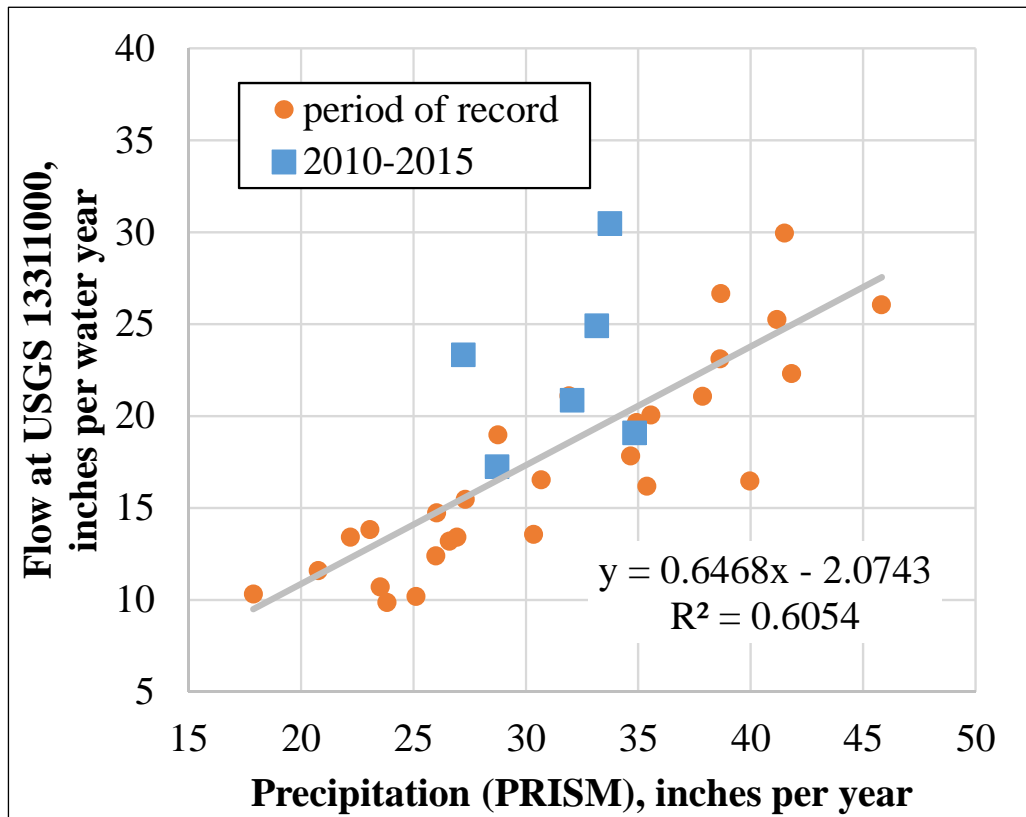

Figure 4.1. Correlation between annual precipitation (PRISM) with water-year average flow at USGS gage 13311000, EFSFSR at Stibnite.

4.3 Groundwater Levels

4.3.1 Measured-Simulated Correlation of Levels

Measured and simulated groundwater levels will be compared on a measured versus simulated scatter plot along with standard statistical measures of the match. Aquifer and streambed parameters will be adjusted to obtain agreement.

4.3.2 Seasonal water-level fluctuations

Measured and simulated groundwater-level hydrographs will be compared and aquifer storage and river recharge parameters adjusted to match the observed range of seasonal water-level fluctuation.

4.3.3 Aquifer Test Results

Aquifer parameters in the vicinity of the Meadow Creek alluvial aquifer will be adjusted to match observation well responses to the December 2013 pumping of the Gestrin airstrip well (BC, 2017). A model simulation representing the period of pumping and recovery will use shorter time steps than the monthly model simulations.

4.4 Historical Dewatering Rates

Historical photographs featuring the Yellow Pine pit (personal communication, Midas Gold, March 31, 2014) such as the one shown on Figure 4.2 show little sign of groundwater inflow to the open pit and no obvious dewatering activity. Aquifer parameters in the vicinity of the Yellow Pine pit will be verified using a simulation of the existing Yellow Pine pit under dewatered conditions.

Figure 4.2. Aerial image of the dewatered, existing Yellow Pine pit (date unknown).

5.0 SENSITIVITY ANALYSES

The sensitivity of model projections to uncertain inputs will be evaluated. Some results will be primarily a function of the Project water balance and not sensitive to model inputs. For other results, sensitivity to aquifer and stream-channel parameters will likely be insignificant compared to sensitivity to the natural variability of annual precipitation.

For still other results, sensitivity to a plausible range of model inputs may be important. Plausible ranges of uncertain model inputs and results will be developed as part of the sensitivity analysis. Some inputs are substantially constrained:

- Combinations of meteoric water balance parameters that do not produce the observed timing and general magnitude of the annual melt are outside of the range.

- Recharge rates or stream channel parameters that do not add enough water to produce the observed level of winter base flow are out of range.

- Aquifer or stream channel parameters that do not produce the observed recession of flows from high-flow season to low-flow season are out of range.

- Aquifer or stream channel parameters that produce results inconsistent with Meadow Creek aquifer testing are out of range.

- Aquifer or stream channel parameters that produce results inconsistent with the observed lack of large groundwater inflow to the historical Yellow Pine pit are out of range.

Results will be presented as a range of plausible outcomes. Sensitivity of model projections to model inputs will be considered together with sensitivity to annual precipitation.

6.0 SUMMARY

This report presented an outline of a quantitative hydrologic model for the upper watershed of the EFSFSR. The model will be used to evaluate the groundwater and surface water flows related to the design of the Project and the assessment of local and downstream effects of the Project.

The study area is a mountain-block watershed. Large annual precipitation falls mainly as winter snow which melts in spring and early summer. Water not consumed by local vegetation becomes flow in the EFSFSR. Groundwater systems in the watershed store melt water and gradually release it to the surface-water system, providing year-round base flow.

The model combines a long-term meteoric water balance with a numerical model of groundwater and surface water flow, computing a distribution of monthly groundwater and surface water flows based on the estimated long-term precipitation pattern.

Calibration of the model to measured groundwater levels and surface-water flows will consider:

- Timing and magnitude of annual high surface flows
- Base flow recession and magnitude of winter low surface flows
- Areal distribution of groundwater levels
- Seasonal fluctuation of groundwater levels
- Meadow Creek aquifer test results
- Approximate history of Yellow Pine open pit dewatering

The calibrated model will be used to evaluate groundwater and surface water levels and flows, and changes to levels and flows. Model results will be presented as ranges of flows for different climatic conditions. The sensitivity of results to a probable range of uncertain model inputs will be evaluated, and the added variability will be considered along with the natural variability due to a range of annual precipitation levels.

7.0 REFERENCES

Brown and Caldwell, 2017, Stibnite Gold Project Water Resource Baseline Summary Report: Consultant report prepared for Midas Gold Idaho Inc., June 2017.

Daly, C., Halbleib, M., Smith, J.I., Gibson, W.P., Doggett, M.K., Taylor, G.H., Curtis, J., and Pasteris, P.A., 2008. "Physiographically-sensitive mapping of temperature and precipitation across the conterminous United States". International Journal of Climatology, DOI: 10.1002/joc.1688.

Hidromas, 2014, Resumen Modelo Hidrológico E Hidrogeológico Conceptual Y Numérico Rio Del Estrecho: consultant's report prepared for Compañía Minera Nevada, March 2014.

HydroGeo, Inc., 2012, Surface water hydrology baseline study for Golden Meadows project: consultant's report prepared by HydroGeo, Inc. for Midas Gold Inc., December 2012.

[IDIH] Instituto Hidráulico San Juan Argentina IDIH, 2006, Proyecto Pascua Lama informe de Impacto Ambiental Estudio Ampliado del Agua: Instituto de Investigaciones Hidráulicas UNSJ, junio 2006.

Jones M., 2004, Modelo Hidrológico de la Cuenca del Río de las Taguas Superior, Apéndice O-1 del Informe Impacto Ambiental del Proyecto Pascua Lama: consultant's report prepared by Michael A. Jones for Knight Piesold Consulting, mayo 2004.

Jones, M.A., 2006, Modelo Hidrológico de la Cuenca del Río Estrecho: consultant's report prepared by Michael A. Jones for Proyecto Pascua-Lama Compañía Minera Nevada, January 2006.

[JSAI] John Shomaker & Associates, Inc., 2016, Nickel Plate Tailings Impoundment Water Balance: consultant's report prepared for Barrick Nickel Plate, 24 p.

Lund, K., 2004, Geologic setting of the Payette National Forest, west-central Idaho: U.S. Geological Survey Professional Paper 1666 (2004), p. 1-44.

McDonald, M. G., and Harbaugh, A.W., 1988, A modular three-dimensional finite-difference ground-water flow model: U.S. Geological Survey, Techniques of Water Resources Investigations, Book 6, Chapter A1, 586 p.

Midas Gold Idaho, Inc (Midas Gold). 2016. *Plan of Restoration and Operations*, Stibnite Gold Project. Valley County, Idaho. September.

Midas Gold. 2017. *Geological Resources Baseline Study*. Stibnite Gold Project. Midas Gold, Inc. Samuel B. Reid and Christopher Dail. May 2017.

SRK, 2012, Groundwater data interim update: letter report prepared by SRK Consulting (Canada) Inc. for Midas Gold Inc., November 15, 2012.

Stewart, D. E., Stewart, E. D., Lewis, R. S., Weppner, K. N., Isakson, V. H., 2016, Geologic Map of the Stibnite Quadrangle, Valley County, Idaho: Idaho Geologic Survey Geologic Map 51, 2 plates, viewed June 29, 2017 at www.idahogeology.org, scale 1:24,000.

Tierra Group International, Ltd., 2013, Golden Meadows pre-feasibility engineering: Climatology data review and path forward: memorandum prepared by Tierra Group International, Ltd. for Midas Gold Inc., December 4, 2013.

Zhan, G., and Shelp, M. L., 2009, Modified Blaney-Criddle method – an empirical approach to estimate potential evaporation using air temperature: Proceedings of Fourth International Conference on Mine Closure, September 9-11, Perth, Australia.